© 2015. Published by The Company of Biologists Ltd | Development (2015) 142, 1159-1168 doi:10.1242/dev.113431

RESEARCH ARTICLE

Tbx6, Mesp-b and Ripply1 regulate the onset of skeletal myogenesis in zebrafish

Stefanie E. Windner[1], Rosemarie A. Doris[1,*], Chantal M. Ferguson[1,*], Andrew C. Nelson[2,*], Guillaume Valentin[3,*], Haihan Tan[2], Andrew C. Oates[3], Fiona C. Wardle[2] and Stephen H. Devoto[1,‡]

ABSTRACT

During embryonic development, the paraxial mesoderm becomes segmented into somites, within which proliferative muscle progenitors and muscle fibers establish the skeletal musculature. Here, we demonstrate that a gene network previously implicated in somite boundary formation, involving the transcriptional regulators Tbx6, Mesp-b and Ripply1, also confers spatial and temporal regulation to skeletal myogenesis in zebrafish. We show that Tbx6 directly regulates *mesp-b* and *ripply1* expression *in vivo*, and that the interactions within the regulatory network are largely conserved among vertebrates. Mesp-b is necessary and sufficient for the specification of a subpopulation of muscle progenitors, the central proportion of the Pax3$^+$/Pax7$^+$ dermomyotome. Conditional ubiquitous expression indicates that Mesp-b acts by inhibiting myogenic differentiation and by inducing the dermomyotome marker *meox1*. By contrast, Ripply1 induces a negative-feedback loop by promoting Tbx6 protein degradation. Persistent Tbx6 expression in Ripply1 knockdown embryos correlates with a deficit in dermomyotome and myotome marker gene expression, suggesting that Ripply1 promotes myogenesis by terminating Tbx6-dependent inhibition of myogenic maturation. Together, our data suggest that Mesp-b is an intrinsic upstream regulator of skeletal muscle progenitors and that, in zebrafish, the genes regulating somite boundary formation also regulate the development of the dermomyotome in the anterior somite compartment.

KEY WORDS: Dermomyotome, Myotome, Segmentation, Maturation, Zebrafish, Heat shock, Protein degradation, Determination front, Wavefront, Gene regulatory network

INTRODUCTION

Skeletal musculature in the vertebrate embryo originates in the paraxial mesoderm, which develops on either side of the neural tube and notochord, and subsequently segments into somites. Segmentation of paraxial mesoderm into somites and myogenesis within each somite are sequentially initiated, starting posterior to the head and progressing towards the tail bud, which simultaneously produces more paraxial mesoderm to elongate the body axis (Buckingham and Vincent, 2009; Oates et al., 2012). How the onset of myogenesis is coordinated with the formation of somites is not yet understood.

[1]Department of Biology, Wesleyan University, Middletown, CT 06459, USA. [2]Randall Division of Cell and Molecular Biophysics, New Hunt's House, King's College London, Guy's Campus, London, SE1 1UL, UK. [3]MRC National Institute for Medical Research, The Ridgeway, Mill Hill, London, NW7 1AA, UK.
*These authors contributed equally to this work

‡Author for correspondence (sdevoto@wesleyan.edu)

Received 2 June 2014; Accepted 27 January 2015

Expression of the paired domain transcription factor *pax3* marks the entry of paraxial mesoderm cells into the myogenic program before their incorporation into a somite (Kusakabe and Kuratani, 2005; Buckingham and Relaix, 2007). Subsequently, Pax3-expressing cells give rise to two spatially segregated myogenic tissues. The dermomyotome, a transient epithelial structure containing proliferative muscle progenitors, is located at the lateral somite surface; the myotome, consisting of differentiated muscle fibers, lies underneath/medial to the dermomyotome. Muscle progenitors retain *pax3* expression and upregulate *pax7*, whereas differentiating muscle fibers downregulate *pax3* and express myogenic regulatory factors like *myoD* and *myf5* (Buckingham and Rigby, 2014).

The zebrafish myotome consists of spatially segregated slow and fast muscle fibers, which are specified in the pre-somitic paraxial mesoderm. First, Hedgehog signaling from the notochord and ventral neural tube induces slow muscle fibers in the adjacent medial paraxial mesoderm (Blagden et al., 1997; Du et al., 1997). Then, immediately before somite boundary formation, Hedgehog and Fgf8 signaling promote differentiation of fast fibers in the *pax3*-expressing lateral paraxial mesoderm, specifically in the posterior half of the future somite (Groves et al., 2005; Hammond et al., 2007). After somite formation, *pax3*-expressing cells in the anterior half of the lateral somite upregulate *pax7* and translocate to the surface of the developing myotome (Hollway et al., 2007; Stellabotte et al., 2007). It is unknown how the onset of *myoD* expression becomes restricted to the posterior half of the lateral somite. Similarly, it is unknown what promotes the development of Pax3$^+$/Pax7$^+$ dermomyotome cells in the anterior half of the lateral somite.

The establishment of anterior and posterior half-somite domains has been studied in the context of segmentation, because the polarized/alternating expression of genes in the pre-somitic mesoderm precedes somite boundary formation (Dahmann et al., 2011). The patterning process begins in the tailbud, where single cells initiate oscillating expression of members of the Her/Hes family of bHLH transcriptional repressors, which are subsequently synchronized among neighboring cells by Delta-Notch signaling (Pourquié, 2011; Oates et al., 2012). Before morphological boundary formation, these oscillations, known as the segmentation clock, are translated into non-oscillating expression of genes specific to either prospective anterior or posterior half-somites (Saga, 2012).

tbx6/fused somites encodes a T-box transcription factor required for the maintenance and readout of these oscillations in the anterior pre-somitic mesoderm, and for the formation of somite boundaries in zebrafish (van Eeden et al., 1996; Nikaido et al., 2002; Oates et al., 2005; Brend and Holley, 2009). We recently discovered that Tbx6 is also required for the development of a subpopulation of dermomyotome cells (Windner et al., 2012). *tbx6* mutants

Development (2015) 142, 1159-1168 doi:10.1242/dev.113431

ectopically upregulate *myoD* in the anterior half-somite, which correlates with a gain in fast fiber nuclei and a loss of the central domain of the $Pax3^+/Pax7^+$ dermomyotome, whereas peripheral (dorsal and ventral) dermomyotome develops normally. These findings suggest that Tbx6 inhibits premature differentiation of dermomyotome cells, and provide an unexpected link between myogenesis and somite boundary formation.

In mouse, expression of the bHLH transcription factor *Mesp2* is induced by the combination of Tbx6 and spatially restricted Notch signaling, specifically in the anterior half of the future somite (Yasuhiko et al., 2006). Mesp2 promotes morphological somite boundary formation via activation of Eph/Ephrin signaling and activates co-repressors of the Ripply family, which terminate the patterning network by negatively regulating Tbx6 function (Nakajima et al., 2006; Takahashi et al., 2010). *mesp* and *ripply* genes are expressed in a Tbx6-dependent manner and also regulate anterior-posterior somite polarity in zebrafish (Sawada et al., 2000; Kawamura et al., 2005); however, it is unknown whether they play a role in myogenesis.

Here, we analyze the Tbx6–Mesp-b–Ripply1 regulatory network in zebrafish and reveal its role at the onset of skeletal myogenesis. We show that both *mesp-b* paralogs and *ripply1* are direct targets of Tbx6. Mesp-b is necessary and sufficient for development of the central domain of the $Pax3^+/Pax7^+$ dermomyotome, similar to Tbx6. Mesp-b inhibits *myoD* and *myf5* expression, and by inducing the dermomyotome marker *meox1* in the anterior half of future somites. By contrast, Ripply1 negatively regulates *mesp-b* expression by eliminating Tbx6 protein. This negative-feedback loop, which is also promoted by Mesp-b, is required for upregulation of *pax3/7* as well as *myoD* and *myf5*, suggesting a Tbx6-dependent inhibition of myogenic gene expression. Our results provide an explanation for the spatially restricted development of myogenic progenitors within the somites, and for the temporal coordination of myogenesis with the formation of somite boundaries.

RESULTS

Tbx6 directly regulates *mesp-b* and *ripply1* expression

Tbx6 is required for the expression of *mesp-b* and *ripply1* in the paraxial mesoderm during somite formation, and for the specification of the central $Pax3^+/Pax7^+$ dermomyotome (Sawada et al., 2000; Kawamura et al., 2005; Windner et al., 2012). At the 10-somite stage (14 h post fertilization), *tbx6* mRNA was highly expressed throughout the anterior pre-somitic mesoderm, and at decreasing levels in the recently formed somites SI-SIII, whereas, surprisingly, Tbx6 protein was downregulated prior to somite formation (Fig. 1A,B). Specifically, Tbx6 protein was reduced in the posterior proportion of S-I and virtually undetectable throughout the S-0 domain (antibody specificity shown in supplementary material Fig. S1). *mesp-ba* and *ripply1* mRNA spatially overlapped with Tbx6 protein (Fig. 1C,D): *mesp-ba* was expressed in two precise stripes in the future anterior half-somite in S-II and S-I; *ripply1* expression was initiated in the future posterior half-somite in S-I, highly upregulated throughout the anterior and posterior of S-0 and SI, and gradually downregulated and restricted to the anterior half in the maturing somites. *myoD* was co-expressed with Tbx6 in the developing slow muscle fibers along the medial somite surface, but did not overlap with Tbx6 in the lateral paraxial mesoderm (Fig. 1E).

We carried out chromatin immunoprecipitation, followed by high throughput sequencing (ChIP-seq) of DNA associated with Tbx6. Because the Tbx6 antibody did not work for ChIP (data not shown), we used a transgenic zebrafish line with heat shock-inducible Myc-tagged Tbx6, *Tg(hsp70l:tbx6^{myc})^{v8}*, that can rescue the *tbx6* mutant phenotype (Windner et al., 2012), and immunoprecipitated with an anti-Myc antibody 1 h after transgene induction. We identified regions of Tbx6 binding in close proximity to the *mesp-ba*, *mesp-bb* and *ripply1* genes (Fig. 1F; supplementary material Table S1), many of which match those found computationally using the T-box consensus motif (Cutty et al., 2012). *De novo* motif discovery showed that the Tbx6^{Myc} *in vivo* binding sequences included the consensus T-box previously identified for T-box proteins in zebrafish and mouse (Kispert and Hermann, 1993; Garnett et al., 2009) (Fig. 1G; supplementary material Table S2). The binding site near the transcriptional start site of *mesp-ba* has been confirmed previously by Kawamura et al. (2008); we confirmed the binding site ~6700 bp upstream of the transcription start site by ChIP-PCR (supplementary material Fig. S2).

Combined, these data suggest that Tbx6 directly regulates the *mesp-b* and *ripply1* genes *in vivo*. The expression of *mesp-b* and *ripply1* precedes the development of dermomyotome cells in the anterior half-somite and fast muscle fibers in the posterior half-somite (Fig. 1H).

Mesp-b is necessary and sufficient for central dermomyotome formation

To test whether *mesp-b* regulates dermomyotome development in the anterior half-somite, we knocked down Mesp-b function using morpholinos (MOs) against both zebrafish paralogs (Mesp-ba and Mesp-bb MOs, henceforth referred to as Mesp-b MO). Knockdown of either Mesp-ba or Mesp-bb alone did not result in a dermomyotome phenotype (data not shown), suggesting functional redundancy between *mesp-b* paralogs. We found that translation-blocking and splice-blocking Mesp-b MOs produced similar phenotypes, and validated the functionality of the splice-blockers by RT-PCR (supplementary material Fig. S3). As previously reported, *ripply1* mRNA was expressed in the pre-somitic mesoderm in Mesp-b morphants; however, expression was not maintained after somite boundary formation (Kawamura et al., 2005) (Fig. 2A).

The dermomyotome marker *meox1* and the myotome marker *myoD* were similarly expressed in pre-somitic mesoderm in control and Mesp-b MO-injected embryos, but showed complementary changes within the somites: in newly formed somites, *meox1* was reduced and *myoD* expanded to the anterior half-somite, whereas in more mature somites, neither mRNA was maintained in the lateral somite (Fig. 2B,C). *myoD* expression in slow muscle progenitors along the medial somite surface was not affected in Mesp-b morphants. The transient upregulation of *myoD* in anterior and posterior half-somites resembled the pattern of *myoD* expression in *tbx6* mutants (van Eeden et al., 1996; Windner et al., 2012), and, together with a downregulation of *meox1*, suggests a loss of dermomyotome and an expansion of fast muscle development.

Indeed, the number of $Pax7^+$ dermomyotome cells was reduced in Mesp-b morphants, specifically in the central domain of the trunk, identical to the dermomyotome phenotype in *tbx6* mutants at the 24-h stage (Fig. 2D-F). The loss of central, but not peripheral, dermomyotome in *tbx6* mutant and Mesp-b knockdown embryos was consistent with the restriction of *mesp-b* expression to the central proportion of the paraxial mesoderm (supplementary material Fig. S4). We conclude that, downstream of Tbx6, Mesp-b is required for central dermomyotome development.

To test whether Mesp-b can rescue central dermomyotome development in the absence of *tbx6*, we created transgenic fish

Development (2015) 142, 1159-1168 doi:10.1242/dev.113431

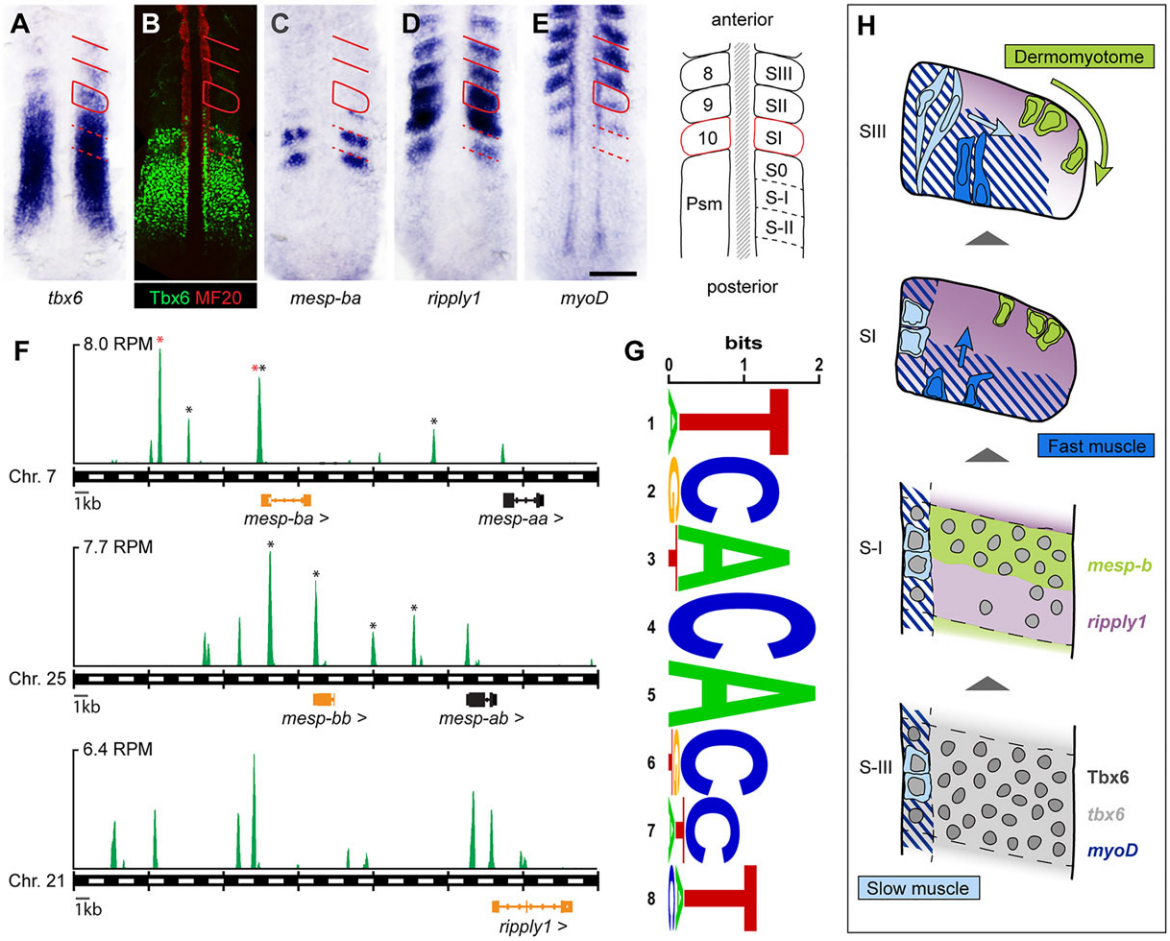

Fig. 1. Tbx6 induces *mesp-b* paralogs and *ripply1* before the onset of myogenesis in lateral paraxial mesoderm. (A-E) Labeling for *tbx6*, *mesp-ba*, *ripply1* and *myoD* mRNAs, and for Tbx6 and myosin heavy chain (MF20) proteins at the 10-somite stage. Unbroken lines indicate most recently formed somites (SI-SIII); dashed lines indicate future somites (S0, S-I, S-II) in the anterior pre-somitic mesoderm (PSM). Scale bar: 100 µm. (F) Anti-Myc immunoprecipitation from *Tg(hsp70l:tbx6^{myc})* embryos 1 h after heat shock and subsequent sequencing reveals Tbx6^{Myc} genomic binding proximal to *mesp-ba*, *mesp-bb* and *ripply1*. Shown are 35-kb windows encompassing significant peaks in reads per million (RPM) (supplementary material Table S1). Black asterisks indicate correspondence with T-box binding sites identified by Cutty et al. (2012). Red asterisks indicate peaks confirmed by ChIP-PCR (supplementary material Fig. S2). (G) Top sequence motif found in Tbx6^{Myc} binding peaks (supplementary material Table S2). (H) Schematic showing spatial and temporal correlation of *tbx6*, *mesp-ba* and *ripply1* expression with the onset of dermomyotome and myotome (slow and fast fiber) development (adapted from Stellabotte and Devoto, 2007).

with a heat shock-inducible promoter driving ubiquitous expression of Myc-tagged Mesp-ba, *Tg(hsp70l:mesp-ba^{myc})*. Transgene expression in *tbx6* mutants during segmentation stages caused an increase in the number of Pax7^{+} central dermomyotome cells at the 24-h stage, and rescued medio-lateral patterning of slow and fast muscle fibers, which is disrupted in *tbx6* mutants (Fig. 2G-K). At the 36-h stage, the number of Pax7^{+} dermomyotome cells and the size of the myotome in transgenic *tbx6* mutants were increased when compared with non-transgenic siblings, and resembled those in wild-type embryos (Fig. 2L-N). Thus, ubiquitous Mesp-ba expression is sufficient to rescue myogenic phenotypes found in *tbx6* mutants (Windner et al., 2012).

tbx6 mutants do not form somite boundaries (*fused somites* phenotype) (van Eeden et al., 1996). By contrast, Mesp-b morphants formed irregular somites (Fig. 2A-C) and showed clearly segmented myotomes, as indicated by expression of the myogenic enhancer factor Mef2 and myosin heavy chain protein (MF20) in differentiated muscle fibers (Fig. 2D-F). Conversely, ubiquitous Mesp-ba expression did not fully rescue somite boundary formation in *tbx6* mutants, but resulted in the formation of partial and irregularly spaced myotome boundaries (Fig. 2M).

Combined, these knockdown and rescue experiments suggest that Mesp-b is necessary and sufficient for central dermomyotome development downstream of Tbx6, but not necessary/sufficient for somite boundary formation.

Mesp-b inhibits myogenic differentiation and promotes dermomyotome development

To further examine the role of Mesp-b in central dermomyotome development, we analyzed the immediate effects of ubiquitous Mesp-ba^{Myc} expression on genes characterizing the onset of dermomyotome development (*meox1*, *pax3*) and myogenic differentiation (*myoD*, *myf5*) in wild-type embryos. Transient overexpression of Mesp-ba led to the opposite effect of Mesp-b knockdown; in *Tg(hsp70l:mesp-ba^{myc})* embryos 15 min after heat shock, the expression of *myoD* and *myf5* in the lateral paraxial mesoderm was downregulated, and the expression of *meox1* was upregulated (Fig. 3A-C; supplementary material Fig. S5). The rapid changes in mRNA levels occurred similarly in all somites, independent of their maturation state, and did not affect the

Development (2015) 142, 1159-1168 doi:10.1242/dev.113431

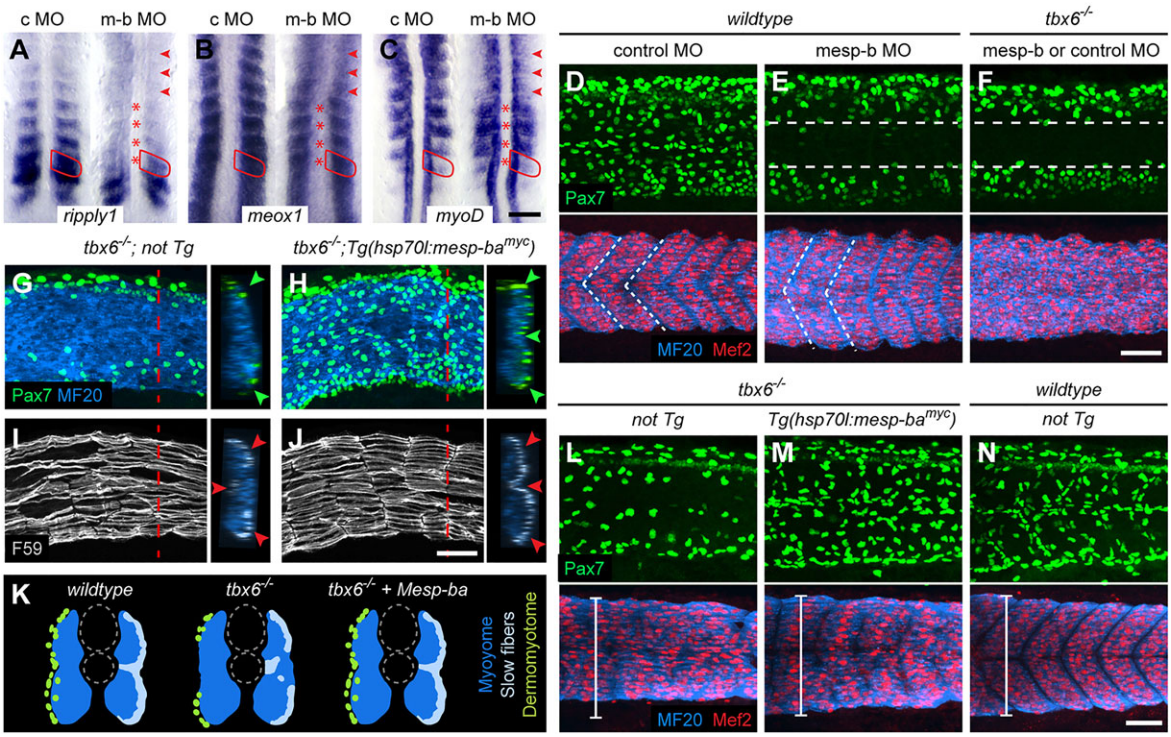

Fig. 2. Mesp-b knockdown recapitulates and Mesp-ba^{Myc} expression rescues dermomyotome phenotype in *tbx6* mutants. (A-F) Control and Mesp-b ATG MO-injected embryos at the 12-somite (A-C) and 24-h (D-F) stage. (A) *ripply1*, (B) *meox1* and (C) *myoD* mRNA expression. Red asterisks indicate most recently formed somites; SI is outlined; red arrowheads indicate downregulation of all three genes in maturing somites. (D-F) Immunolabeling showing dermomyotome (Pax7, green) and corresponding myotome (MF20, blue; Mef2, red). Mesp-b morphants phenocopy *tbx6* mutant dermomyotome but form somites similar to wild type; Mesp-b knockdown has no effect in *tbx6* mutants. Dashed lines indicate central dermomyotome domain (top) and somite boundaries (bottom). (G-J,L-N) Non-transgenic and *Tg(hsp70l:mesp-ba^{myc}) tbx6* mutants heat-shocked at the 12-somite stage. (G-J) Transgenic embryos show increase in Pax7^{+} dermomyotome cells (G,H) and rescued patterning of slow muscle fibers (F59, gray) within the myotome (MF20, blue) (I,J). (K) Schematic illustrating rescue of *tbx6* mutant phenotypes by transient Mesp-ba^{Myc} expression. (L-N) Transgenics develop larger myotomes (brackets), and show partially rescued myotome boundaries, similar to wild type. Scale bars: 100 µm in C; 50 µm in F,J,N.

developing slow muscle fibers in the medial paraxial mesoderm. This suggests that specific effects on myogenic marker genes are immediately downstream of Mesp-b.

pax3 is expressed in myogenic progenitors in future anterior and posterior somite domains before being restricted to the developing dermomyotome (Groves et al., 2005). We could not detect differences in *pax3* mRNA levels between transgenic embryos and non-transgenic siblings at this stage (Fig. 3D), indicating that Mesp-ba does not directly regulate *pax3* expression, and that the total population of dermomyotome and fast muscle fibers was not altered by ubiquitous Mesp-ba expression.

Six hours post heat shock (24-somite stage), the dorsal-to-ventral extent of *myoD* expression was reduced in *Tg(hsp70l:mesp-ba^{myc})* embryos, whereas *meox1* was still upregulated, particularly in somites formed during transgene expression (Fig. 3E,F). Smaller myotomes in *Tg(hsp70l:mesp-ba^{myc})* embryos showed a deficit specifically in differentiated fast muscle fibers, which expressed myosin heavy chain protein (MF20) and low levels of Mef2 in non-transgenic siblings (Fig. 3G,H). By contrast, slow muscle fiber differentiation was comparable in transgenic and non-transgenic embryos.

Nine hours post heat shock (24-h stage), *Tg(hsp70l:mesp-ba^{myc})* embryos had an increased number of mature, Pax7^{+} dermomyotome cells (Fig. 3I,J), which spatially correlated with the decrease in *myoD* expression 6 h after heat shock (Fig. 3E). However, myotome sizes were similar in transgenic and non-transgenic embryos at this stage. The recovery of fast muscle indicates that dermomyotome-derived myogenesis is not disrupted in *Tg(hsp70l:mesp-ba^{myc})* embryos and compensates for the initial muscle deficit.

Together, these results show that transient ubiquitous expression of Mesp-ba causes immediate changes in dermomyotome and myotome marker gene expression, which correlate with an inhibition of fast muscle development and an increase in the number of Pax7^{+} dermomyotome cells.

Ripply1 is necessary and sufficient for the elimination of Tbx6 protein

To determine whether Ripply1 negatively regulates Tbx6 protein, as seen in the context of somite formation in mouse (Takahashi et al., 2010), we knocked down Ripply1 function using MOs. As previously shown (Kawamura et al., 2005), knockdown of Ripply1 caused a loss of somite boundary formation, similar to the segmentation phenotype seen in *tbx6* mutants.

In Ripply1 morphants during segmentation stages, *tbx6* mRNA and protein were present at high levels throughout the paraxial mesoderm (Fig. 4A,B). Reflecting the expression of Tbx6 in Ripply1 morphants, both *mesp-b* paralogs were expressed in one to three stripes in the presomitic mesoderm (PSM), similar to their expression in control embryos, but remained upregulated in the anterior paraxial mesoderm (Fig. 4C,D). These expression patterns are consistent with previous work (Kawamura et al., 2005), and suggest that Ripply1 restricts the expression of Tbx6 to the presomitic mesoderm, where spatially restricted co-regulators further confine *mesp-b* expression to the future anterior half-somite.

Development (2015) 142, 1159-1168 doi:10.1242/dev.113431

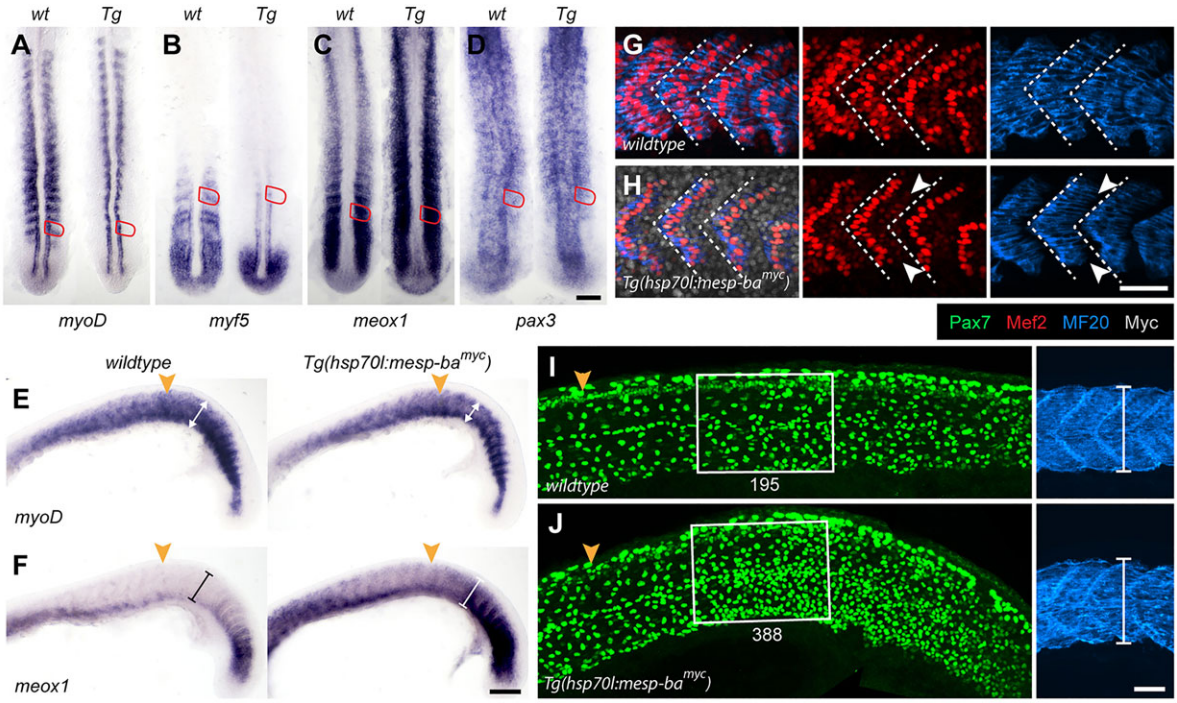

Fig. 3. Mesp-ba^{Myc} inhibits fast fiber differentiation and promotes dermomyotome development. *Tg(hsp70l:mesp-ba^{myc})* embryos and wild-type siblings 1 h (A-D), 6 h (24-somite stage) (E-H) and 9 h (24-h stage) (I,J) after the end of heat shock. (A-D) Transgenic embryos show downregulation of *myoD* (A) and *myf5* mRNA (B) in the lateral paraxial mesoderm, and upregulation of *meox1* (C), but no difference in *pax3* (D). Most recently formed somite SI is outlined. (E,F) *myoD* expression shows smaller myotomes (E, brackets) in somites formed after heat shock (orange arrowhead); *meox1* mRNA is upregulated throughout those somites (F, brackets). (G,H) In transgenic embryos (Myc^{+}, gray), the number of slow muscle nuclei (Mef2, bright red) is similar to wild type, but fast fiber nuclei (Mef2, faint red) and myosin heavy chain protein (MF20, blue) are reduced (arrowheads). (I,J) Immunolabeling shows increase in Pax7^{+} dermomyotome cells (green) in *Tg(hsp70l:mesp-ba^{myc})* embryos (number indicated); boxed areas show underlying myotomes (MF20, blue) on the right. Orange arrowheads mark last somite formed before heat shock. Scale bars: 100 µm in D,F; 50 µm in H,J.

Ubiquitous expression of Ripply1 in *Tg(hsp70l:ripply1^{myc})* embryos eliminated Tbx6 protein in the pre-somitic mesoderm, while only slightly reducing *tbx6* mRNA (Fig. 4E,F), thus supporting a role for Ripply1 in regulating Tbx6 at the protein level. Consistent with a lack of Tbx6 protein, *mesp-ba* expression was downregulated and *myoD* mRNA was upregulated in transgenic embryos (Fig. 4G; supplementary material Fig. S6A). To independently test whether Ripply1 promotes degradation of Tbx6 protein we injected either control or Ripply1 MOs into *Tg(hsp70l:tbx6^{myc})^{v8}* embryos, heat-shocked for 30 min during segmentation stages and fixed 15 min post heat shock (supplementary material Fig. S6B). In Ripply1 morphants, endogenous Tbx6 protein was present in paraxial mesoderm cells along the entire anterior-posterior axis; transgene expression led to additional Tbx6 protein in the notochord and surface ectoderm. Control MO-injected embryos also show high levels of Tbx6 expression in the notochord and surface ectoderm, but not in the paraxial mesoderm. Thus, Tbx6 protein is immediately removed specifically from the paraxial mesoderm in a Ripply1-dependent manner.

Mesp-ba induces negative feedback

Ubiquitous Mesp-ba expression in *Tg(hsp70l:mesp-ba^{myc})* embryos increased *ripply1* mRNA levels in wild type and induced *ripply1* expression in *tbx6* mutants (Fig. 4H,I), suggesting that Tbx6 regulation of *ripply1* is also mediated by Mesp-b in zebrafish, as in mouse (Morimoto et al., 2007).

In *Tg(hsp70l:mesp-ba^{myc})* embryos after heat shock, Mesp-ba^{Myc} protein levels remained high throughout the paraxial mesoderm for several hours after transgene induction (Fig. 3H). However, *mesp-ba* mRNA was highly upregulated only in the intermediate mesoderm and neural tube of transgenic embryos, whereas mRNA levels in the paraxial mesoderm were reduced, including expression from the endogenous *mesp-ba* gene (Fig. 4J). Conversely, knockdown of Mesp-b function caused an increase in *mesp-b* mRNA expression (Fig. 4K).

Together, these data suggest that Mesp-b downregulates its own mRNA, possibly via induction of Ripply1 and consequent Tbx6 protein degradation.

Ripply1 function is required for maturation and fast muscle fiber differentiation

In contrast to transient upregulation of Mesp-ba in *Tg(hsp70l:mesp-ba^{myc})* embryos, knockdown of Ripply1 causes continuously high levels of *mesp-b* expression (Fig. 3 and Fig. 4C,D) (Kawamura et al., 2005). We hypothesized that this would amplify the myogenic phenotypes seen in transgenic embryos and further increase the number of Pax7^{+} dermomyotome cells.

Ripply1 knockdown did not have an effect in *tbx6* mutants (supplementary material Fig. S7A), indicating that Ripply1 acts mainly through elimination of Tbx6 protein. Similar to *Tg(hsp70l:mesp-ba^{myc})* embryos after heat shock, Ripply1 knockdown reduced expression of *myoD* in the lateral paraxial mesoderm (Fig. 3A; supplementary material Fig. S7B). Surprisingly, knockdown of Ripply1, although causing high levels of Tbx6, *mesp-b* and *meox1*, resulted in downregulation of *pax3* mRNA (Fig. 5A,B; supplementary material Fig. S7C). In wild type, *pax3* is expressed at the beginning of both dermomyotome and fast muscle development (Groves et al., 2005); thus, a lack of *pax3*

Development (2015) 142, 1159-1168 doi:10.1242/dev.113431

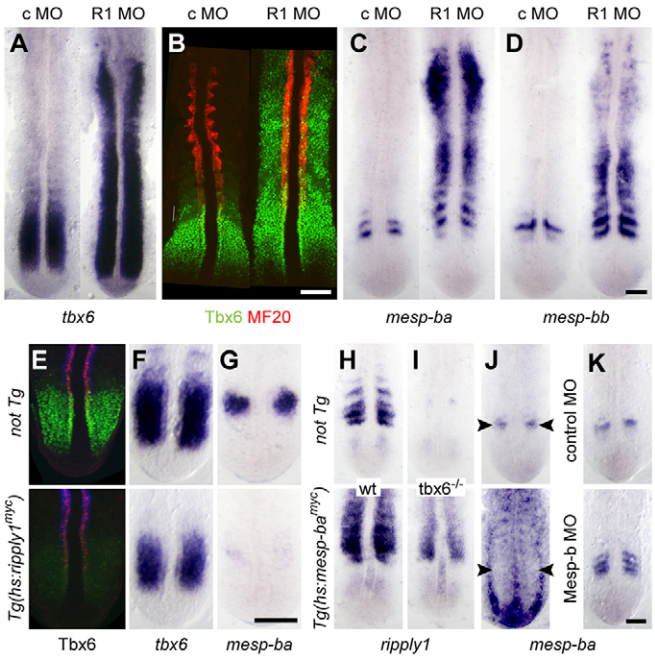

Fig. 4. Ripply1 terminates *tbx6* and *mesp-b* expression in the pre-somitic mesoderm. (A-D) Control and Ripply1 MO-injected embryos at the 12-somite stage labeled for *tbx6* (A, mRNA; B, protein), and *mesp-ba* (C) and *mesp-bb* mRNA (D). All markers are upregulated in the absence of Ripply1. MF20 (B, red) labels slow muscle progenitors. (E-G) *Tg(hsp70l:ripply1^{myc})* embryos and non-transgenic sibling 0.5 h (E) and 1 h (F,G) post heat shock. Transgenics lose expression of Tbx6 protein (E) and *mesp-ba* mRNA (G), *tbx6* mRNA is only slightly reduced (F). (H-J) *Tg(hsp70l:mesp-ba^{myc})* embryos and non-transgenic siblings 1 h post heat shock. Ubiquitous expression of Mesp-ba leads to upregulation of *ripply1* mRNA in wild type and *tbx6* mutants (H,I). *mesp-ba* mRNA is not ubiquitously upregulated after *Tg(hsp70l:mesp-ba^{myc})*: levels are low in the paraxial mesoderm, endogenous *mesp-ba* expression (arrowheads) is downregulated (J). (K) Control and Mesp-b MO-injected embryos labeled for *mesp-ba* mRNA. Scale bars: 100 µm.

expression indicates a general inhibition of myogenesis in the lateral paraxial mesoderm.

We did not observe Pax7$^+$ dermomyotome cells or differentiated fast muscle fibers in the presence of Tbx6 protein (Fig. 5C,D; supplementary material Fig. S7D). The elimination of Tbx6 protein in Ripply1 morphants took about 8 h, compared with 30 min in the presence of Ripply1, but similarly occurred in an anterior-to-posterior progression. At the 22-somite stage, Tbx6 protein had disappeared from the anterior trunk of Ripply1 morphants, but was still present in the posterior half of the embryo (Fig. 5C). At the same time, the first mature Pax7$^+$ dermomyotome cells appeared in the anterior trunk (Fig. 5D). In the first ~6 somites, which develop independently of Tbx6 function (Windner et al., 2012), *tbx6*, *mesp-b* and *meox1* expression remained elevated for a longer period, and Pax7 expression was further delayed (Fig. 4A,C,D; data not shown).

At the 24-h stage, ectopic *tbx6* was restricted to the most recently formed somites in the tail, whereas *pax3* and *pax7* were highly upregulated throughout the anterior and posterior trunk in Ripply1 morphants (Fig. 5E-G). Immunolabeling confirmed a dramatic increase in the number of Pax7$^+$ dermomyotome cells, most prominent in the central domain of the trunk (Fig. 5H,I). Fast muscle differentiation was completely inhibited prior to upregulation of Pax7, whereas slow muscle fibers differentiated but remained in a position adjacent to the notochord (Fig. 5J,K; supplementary material Fig. S7E). This indicates that knockdown of Ripply1 leads to the induction of dermomyotome development throughout the lateral paraxial mesoderm, at the expense of fast muscle formation, and raises the possibility that, in the absence of Ripply1, fast muscle fibers are exclusively derived from Pax7$^+$ dermomyotome cells.

Combined, these results suggest that continuous expression of Tbx6 and/or Tbx6-dependent genes inhibits myogenesis in the lateral paraxial mesoderm. The Ripply1-dependent elimination of Tbx6 protein prior to somite formation restricts dermomyotome development to anterior half-somites, which facilitates fast muscle differentiation in posterior half-somites.

DISCUSSION

We have explored a gene regulatory network in zebrafish that regulates some of the earliest steps in embryonic myogenesis. Our results significantly extend previous work on the interactions between *tbx6*, *mesp-b* and *ripply1*, and introduce novel roles for Mesp-b and Ripply1 in the specification and maturation of dermomyotome and myotome, respectively. We propose a model that explains how the readout of genes associated with segmentation leads to the spatially restricted specification of myogenic progenitors within the somites, and to the temporal coordination of myogenesis with the formation of somite boundaries (Fig. 6).

Molecular interactions between *tbx6*, *mesp-b* and *ripply1*

Our data suggest that Tbx6 directly regulates the expression of both *mesp-b* paralogs *in vivo* (see also Kawamura et al., 2008; Cutty et al., 2012). Binding of Tbx6 to the *mesp-b* promoter and the functional relevance of this interaction have been demonstrated in other vertebrate models, including medaka (Terasaki et al., 2006), *Xenopus* (Tazumi et al., 2008) and mouse (Yasuhiko et al., 2006, 2008), suggesting that this interaction is conserved. Mesp genes are expressed in one to three precise bands prior to somite boundary formation (Saga et al., 1997; Sawada et al., 2000). The restriction of *mesp-b* expression to the anterior half of future somites in mouse depends on the spatially restricted overlap of Tbx6 with active Notch signaling (Saga, 2012). Oscillating Notch activity is a fundamental component of the segmentation clock, also in zebrafish (Oates et al., 2012). Whether the restricted expression of zebrafish *mesp-b* represents a direct output of the segmentation clock is not known.

We provide the first evidence that Tbx6 directly regulates the expression of the transcriptional co-repressor *ripply1*. We also demonstrate that Mesp-ba can induce *ripply1* in the absence of Tbx6, which is in accordance with studies showing direct activation of the orthologous mouse *Ripply2* by Mesp2 (Morimoto et al., 2007). Further, we show that Mesp-b is not required for the expression of *ripply1* in the anterior PSM but is required for the maintenance of *ripply1* expression in the somites. Together, these results indicate that Tbx6 induces *ripply1* expression in the pre-somitic mesoderm, whereas Mesp-b promotes continued expression within the somites. Our data do not indicate whether Mesp-ba regulation of *ripply1* in zebrafish is direct or indirect.

We show that Ripply1 is necessary and sufficient for the elimination of Tbx6 protein prior to somite formation in zebrafish. Whether this is by ubiquitin-dependent protein degradation, as it is in mouse, remains to be determined (Oginuma et al., 2008; Takahashi et al., 2010). Ripply proteins recruit Groucho/TLE co-repressors to repress Tbx-mediated transcription of *mesp* genes in zebrafish and *Xenopus* (Kondow et al., 2007; Kawamura et al., 2008). Thus, Ripply family members might suppress Tbx6 function in multiple ways. The Ripply1-dependent inhibition of Tbx6 function restricts the activation

Development (2015) 142, 1159-1168 doi:10.1242/dev.113431

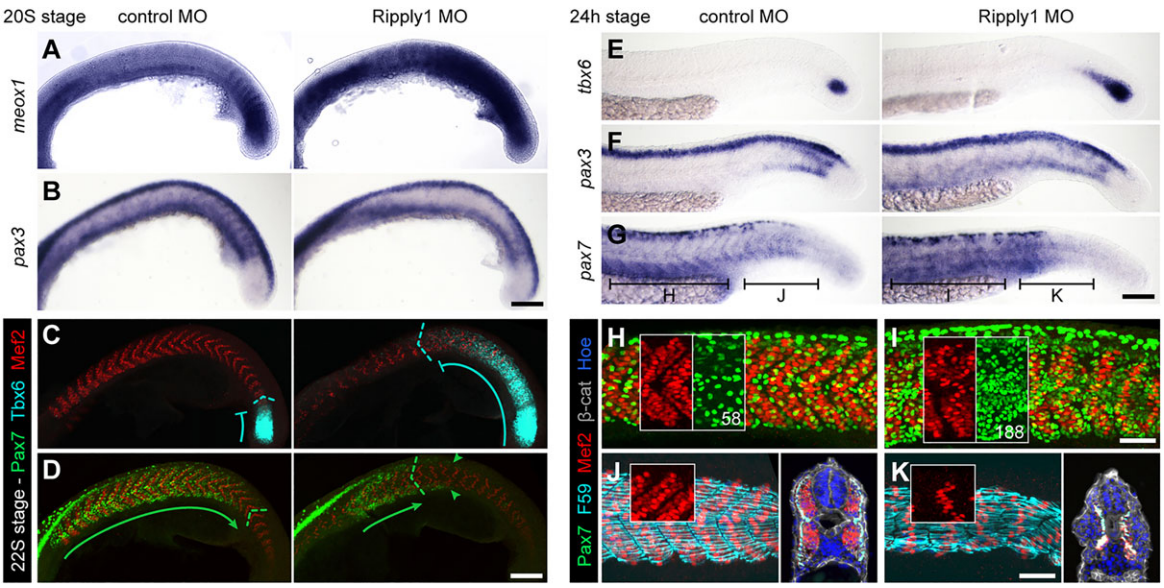

Fig. 5. Ripply1 knockdown inhibits fast muscle development, dermomyotome maturation is delayed. Control and Ripply1 morphants at the 20-somite (A,B), 22-somite (C,D) and 24-h stage (E-K). (A,B) Ripply1 morphants show upregulation of *meox1* (A) and downregulation of *pax3* (B) mRNA. (C,D) In control embryos, Tbx6 is restricted to pre-somitic mesoderm, Pax7$^+$ dermomyotome cells populate somites 1-18; in Ripply1 morphants, Tbx6 protein is expanded into the posterior trunk, Pax7$^+$ cells are restricted to somites ~7-14 (D). The Pax7 and Tbx6 expression domains (green and cyan lines, respectively) do not overlap; the dorsal and ventral domains of the trunk develop faster than the central domain (arrowheads). (E-G) At 24 h, *tbx6* mRNA expression is only slightly expanded in Ripply1 morphants (E); *pax3* (F) and *pax7* (G) are highly upregulated. (H,I) Immunolabeling shows an increase in Pax7$^+$ dermomyotome cells in Ripply1 morphants. Boxes separately show Mef2$^+$ (red) and Pax7$^+$ nuclei (green, number indicated). (J,K) In wild type, slow muscle fibers (F59, cyan) are found lateral to fast fibers; Ripply1 morphants completely lack fast fibers (red, on cross-sections in J,K), slow fibers lie adjacent to the axial structures. β-catenin labels cell membranes, Hoechst all nuclei. Axis levels of images in H-K are indicated in G. Scale bars: 100 µm in B,D,G; 50 µm in I,K.

of *mesp-b* genes to the pre-somitic mesoderm; additional negative feedback might be involved in the rapid downregulation of *mesp* mRNA before somite boundary formation.

Mesp-b regulates dermomyotome development and myotome patterning

The Tbx6-dependent expression of *mesp-b* genes precedes the upregulation of the dermomyotome markers *pax3/7* in space and time (Fig. 6A,B). Pax3 is expressed throughout the lateral paraxial mesoderm immediately before somite boundary formation. The developing dermomyotome cells in the anterior half of the lateral somite maintain *pax3*, and subsequently express *pax7*, whereas downregulation of pax3 and activation of *myoD* and *myf5* leads to differentiation of fast muscle fibers (Groves et al., 2005; Devoto et al., 2006). Signaling molecules, including Fgf8, regulate the onset of *myoD* expression, but not its spatial restriction to the posterior half of the lateral somite (Groves et al., 2005). We propose that *mesp-b* genes promote dermomyotome development in the anterior half-somite.

tbx6 mutants, which do not express *mesp-b*, upregulate *myoD* in the lateral paraxial mesoderm without spatial restriction (van Eeden et al., 1996). This phenotype correlates with an increase in fast fiber nuclei and a decrease in Pax3$^+$/Pax7$^+$ dermomyotome cells, whereas the total number of myogenic nuclei remains the same, thus suggesting ectopic development of fast muscle at the expense of dermomyotome cells in *tbx6* mutants (Windner et al., 2012). Here, we show that *mesp-b* is not expressed in the dorsal and ventral periphery of the somite, and that *mesp-b* morphants recapitulate the specific loss of central dermomyotome seen in *tbx6* mutants, whereas Mesp-ba overexpression rescues the dermomyotome and myotome phenotypes in *tbx6* mutants. Thus, *mesp-b* gene expression regulates the establishment of the central dermomyotome cell population downstream of Tbx6. Normal development of peripheral dermomyotome in *tbx6* mutants and Mesp-b morphants suggests different genetic regulation; whether peripheral dermomyotome cells have a different developmental origin remains to be determined.

We demonstrate that Mesp-b expression immediately upregulates the dermomyotome marker *meox1* and inhibits the expression of *myoD* and *myf5*, specifically in the lateral paraxial mesoderm. Genome-wide transcriptional analysis after Mesp1 induction in mouse cell culture has shown that Mesp1 rapidly activates and represses specific sets of target genes, and thus acts as a key regulatory switch during cardiovascular progenitor cell specification (Bondue et al., 2008). Similarly, we suggest that *mesp-b* genes in the paraxial mesoderm act as an intrinsic determinant for the establishment of the central dermomyotome cell population by activating dermomyotome genes, while at the same time repressing genes promoting the alternative cell fate, the fast myotome. Thus, ubiquitous expression of *mesp-b* in Ripply1 morphants leads to widespread dermomyotome development and completely inhibits fast muscle differentiation throughout the paraxial mesoderm. However, we show that *mesp-b* genes do not immediately promote *pax3/7* expression, which is consistent with *in vivo* analyses placing *pax* genes downstream of *meox1* gene function (Mankoo et al., 2003), but could also indicate that *mesp-b* and *pax3* genes synergistically regulate dermomyotome development.

Taken together, our data provide an explanation for the initial pattern of dermomyotome and fast muscle progenitors in the zebrafish somites. Whether the Mesp-dependent regulation of myogenesis is conserved in vertebrates remains to be determined. In mouse, it has been suggested that *mesp* genes regulate the ability of cells to contribute to the dermomyotome by affecting the process of epithelialization (Takahashi et al., 2005). Thus, it is

Development (2015) 142, 1159-1168 doi:10.1242/dev.113431

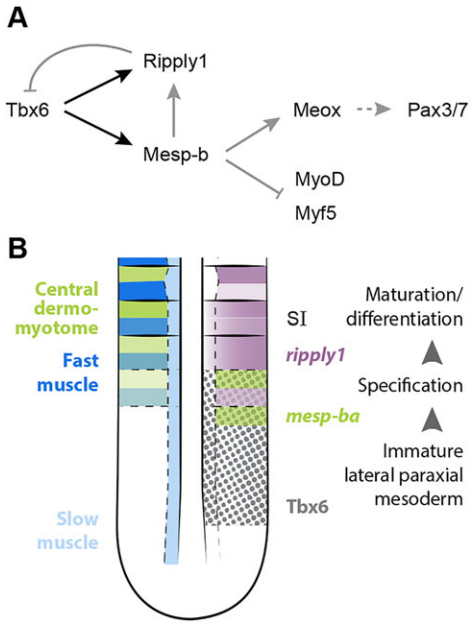

Fig. 6. Gene network regulating specification and maturation of myogenic progenitors. (A) Proposed interactions between Tbx6, Mesp-b and Ripply1 leading to specification of central dermomyotome progenitors (*meox1*, *pax3/7* expression) and inhibition of myogenic differentiation (*myoD* and *myf5* expression). Black lines represent direct interactions shown in this study; gray lines indicate missing evidence for direct interaction; dashed line indicates direct or indirect interactions. (B) Spatial and temporal correlation between development of different myogenic cell populations (left side) and expression of Tbx6 protein and *mesp-ba* and *ripply1* mRNA (right side). Tbx6 expression characterizes immature cells in the lateral paraxial mesoderm prior to boundary formation (SI); Mesp-b specifies central dermomyotome cells in the future anterior half-somite, Ripply1 promotes maturation of dermomyotome and differentiation fast muscle progenitors.

possible that Mesp target genes effect dermomyotome development in various ways, including morphological changes in the paraxial mesoderm.

Slow muscle fibers are induced by Hedgehog signaling from notochord and ventral neural tube in the medial paraxial mesoderm and start differentiating prior to and independent of Tbx6 expression (van Eeden et al., 1996; Blagden et al., 1997; Du et al., 1997; Windner et al., 2012). Slow fibers are not displaced to the lateral somite surface in Ripply1 morphants, in which dermomyotome maturation is delayed, nor in *tbx6* mutants, in which dermomyotome differentiates prematurely into fast muscle. Thus, the translocation of slow fibers depends on properly timed specification and maturation of dermomyotome and fast fibers in the lateral somite. Although Mesp-b expression can rescue the slow fiber phenotype in *tbx6* mutants, it remains to be determined whether Mesp-b affects myotome patterning directly by regulating muscle progenitor translocation, and/or indirectly by regulating the balance between dermomyotome and fast muscle, which could subsequently shape the somite.

Mesp-b and somite boundary formation

Mesp gene expression reliably marks the position of future somite boundaries in the anterior pre-somitic mesoderm and is implicated in regulating somite boundary formation via induction of components of the Eph signaling pathway (Nakajima et al., 2006; Dahmann et al., 2011). The role of Mesp genes in segmentation is well established in mouse (Saga, 2012); however, only *mesp-1/mesp-2* double knockout leads to the complete loss of morphological somite boundaries (Oginuma et al., 2008). We find that irregular somite boundaries persist following knockdown of *mesp-b* in zebrafish (see also Akiyama et al., 2014). We suggest that this might reflect a functional redundancy with *mesp-a* genes, which show similar expression patterns and regulation (Sawada et al., 2000; Cutty et al., 2012). Conversely, transient ubiquitous expression of Mesp-ba is insufficient to completely rescue somite formation in *tbx6* mutants, suggesting that segmental/polarized expression of *mesp* and/or other genes downstream of Tbx6 is required for proper somite boundary formation. The identification of Mesp-b target genes will provide insights into whether the different cellular processes attributed to *mesp* genes result from one or multiple pathways of gene activation.

Ripply1 promotes maturation of myogenic progenitors

Ripply1 is expressed in the future anterior and posterior half-somites prior to boundary formation and negatively regulates Tbx6 and *mesp-b* expression (Kawamura et al., 2005; this study). Our results show that Tbx6 protein has to be removed for the expression of *pax3/7* and *myoD* in the lateral paraxial mesoderm, indicating that Tbx6 and/or Tbx6-dependent genes inhibit maturation of myogenic cells. Downstream of Tbx6, Mesp-ba promotes dermomyotome development but does not immediately promote *pax3* expression, raising the possibility that *mesp* genes are among the Tbx6 targets that have to be downregulated for dermomyotome maturation. A similar mechanism has been shown in cell culture studies, in which transient expression of Mesp1 promotes the differentiation of cardiac progenitors, whereas continuous expression inhibits it (Bondue et al., 2008). We suggest that, by promoting Tbx6 protein degradation, Ripply1 triggers maturation of myogenic progenitors in the lateral paraxial mesoderm (Fig. 6).

In the context of somite boundary formation, the region in the anterior paraxial mesoderm where pre-somitic mesoderm markers are downregulated and somite-specific markers are induced has been termed the determination front/wavefront (Dubrulle et al., 2001). The molecular changes occurring at the front determine the position of future somite boundaries, and include arrest of the segmentation clock and induction of stable expression of genes characterizing future anterior and posterior half-somites (Holley, 2007; Aulehla and Pourquié, 2010; Oates et al., 2012). The appropriate axial position of the front is influenced by signaling gradients: Fgf and Wnt signaling from the tailbud and retinoic acid signaling from the maturing somites (Aulehla and Pourquié, 2010). In zebrafish, *ripply1* expression is directly promoted by retinoic acid (Moreno et al., 2008), and thus constitutes a direct readout of the determination front. We propose that the Ripply1-dependent degradation of Tbx6 protein participates in the developmental switch occurring at the determination front, triggering the morphological segmentation of the paraxial mesoderm, as well as the formation of dermomyotome and myotome.

Although the major components of the determination front are conserved across different vertebrate models, some of the molecular mechanisms seem to be species-specific (Moreno et al., 2008). Future work will determine whether the inhibition of Tbx6 is a conserved feature of the front and coordinates the onset of myogenesis with somite boundary formation also in other vertebrates.

MATERIALS AND METHODS

Animals

All animal experiments were undertaken according to protocols approved by the Wesleyan University Animal Care and Use Committee, assurance number A3956-01.

Development (2015) 142, 1159-1168 doi:10.1242/dev.113431

Zebrafish, transgenesis, heat shock

We used wild-type zebrafish (*Danio rerio*) and the *ti1* or *te314a* allele of *fss/tbx6* mutants, each of which behaves as a null (Nikaido et al., 2002). We detected no differences between wild type and heterozygote *tbx6* mutants, and for readability refer to heterozygous embryos as wild type. We used the *Tg(hsp70l:tbx6^{myc})^{v8}* line and generated stable transgenic lines, using full-length *mesp-ba*, *mesp-bb* (Cutty et al., 2012) and *ripply1* (Kawamura et al., 2005) cDNAs, and gateway cloning as previously described (Kwan et al., 2007; Villefranc et al., 2007; Windner et al., 2012). All plasmids were verified by sequencing. Heat shocks were performed as previously described (Windner et al., 2012), for 1 h at 37°C, unless stated otherwise. Transgenics were identified using anti-cMyc antibody labeling or PCR genotyping. Embryos were cared for using standard procedures (Westerfield, 1995).

Generation of anti-Tbx6 monoclonal antibody

8 µg of a Tbx$_{6327-545}$ peptide fused to GST was injected into Balb/c mice; sera were screened via ELISA. Each antiserum with a positive signal was further tested for tissue-specific binding in 15-somite stage wild-type and *tbx6* mutant embryos. Hybridoma cell lines were produced from one mouse; antibodies were purified from the supernatants. The antibody with highest signal-to-noise ratio was used for experiments (Clone: A83-1, IgG1).

Morpholino (MO) knockdown and RT-PCR

MOs (GeneTools) were resuspended to obtain 1 µM stock solutions, and diluted 1:5 before co-injection with p53 MO into the yolk at the 1-cell stage. MO sequences are included in supplementary material Table S3.

For RT-PCR, embryos were injected with Mesp-ba or Mesp-bb splice-blocking and p53 MOs; total RNA was extracted from ∼50 embryos at bud stage with TRIzol reagent (Life Technologies), with additional RQ1 DNase I treatment (Promega). cDNA was produced using GoScript Reverse Transcriptase (Promega), primers used for PCR are shown in supplementary material Table S3.

In situ hybridization, immunocytochemistry, imaging

Fixations, whole-mount RNA *in situ* hybridization and immunohistochemistry were carried out as previously described (Barresi et al., 2000; Patterson et al., 2010; Windner et al., 2012). Antibodies and RNA probes used are listed in supplementary material Table S3. Images of immunolabeled whole-mounts were taken with a Zeiss LSM510 confocal microscope, and confocal *z*-stacks were flattened. Cryostat cross-sections and *in situ* hybridization samples were imaged on a Zeiss Axioplan compound microscope, and on a Leica stereomicroscope, respectively. Embryos at 20-somite (19-h) stage and older are shown in lateral view, dorsal up, anterior left; younger stages are in dorsal view, anterior up.

ChIP-seq

Tg(hsp70l:tbx6^{myc}) and wild-type embryos were heat-shocked at the 10-somite stage, and fixed 1 h later. ChIP for 2000 embryos per replicate, using 10 µg goat anti-Myc tag antibody (Abcam, ab9132), was carried out as in Wardle et al. (2006), with the exception that purified immunoprecipitated DNA was directly prepared for Illumina sequencing using the TruSeq DNA sample prep kit, with DNA adapters diluted 1:100. Paired-end sequencing of ChIP and their matched input samples were sequenced on an Illumina HiSeq. Duplicate ChIP-seq experiments were performed for *Tg(hsp70l:tbx6^{myc})* and a single control experiment in wild-type embryos.

To define Tbx6^{Myc} binding sites, paired end sequence fragments with unique outer coordinates were mapped to the danRer7 genome build using Bowtie (Langmead et al., 2009) with the following parameters: -5 3 -3 30 –n 3 –y –k 2 –m 2 –best. Peaks were called for each ChIP sample relative to their paired input sample using MACS (Zhang et al., 2008) with the following parameters: –gsize 1.3e+9 –tsize 67 -mfold 8 –pval 5e-10 for Tbx6^{Myc} ChIP samples and –mfold 4 for the wild-type Myc tag control ChIP. Reported peaks are present in both *Tg(hsp70l:tbx6^{myc})* ChIP-seq experiment and absent in the wild-type control. Motif analysis was performed using Weeder v1.4.2 with default parameters (Pavesi et al., 2006), except that both strands were processed; Tbx6^{Myc} binding peaks which were significant in both experiments were used. All ChIP-seq data are stored in NCBI Gene Expression Omnibus under the accession number GSE57332.

T-box identification

For identification of potential T-boxes within genomic regions represented in Fig. 1F, a modified version of the Perl scripts in the TFBS suite was used (Lenhard and Wasserman, 2002) to identify matches to the position frequency matrix generated by Weeder v1.4.2 (see above).

Acknowledgements

The ripply1 cDNA was kindly provided by Shinji Takada. The Tbx antibody project was started by Lola Bajard.

Competing interests

The authors declare no competing or financial interests.

Author contributions

S.E.W. and S.H.D. designed the study, S.E.W. carried out most experiments with help from C.M.F. R.A.D. assembled plasmids for transgenics, carried out ChIP-PCR and provided embryos for ChIP-seq. A.C.N. designed and carried out IP, library preparation for the ChIP-seq and computational analysis. G.V. created and validated the anti-Tbx6 monoclonal antibody. H.T. designed Mesp-b MOs and performed RT-PCR validation. A.C.O. directed anti-Tbx6 antibody production. F.C.W. directed ChIP-seq experiments and Mesp-b MO design/validation. A.C.O. and F.C.W. provided ideas and discussion throughout the study. S.E.W. and S.H.D. wrote the manuscript with contributions from all other authors.

Funding

Our work was supported by the National Institutes of Health (NIH) [R01 HD37509]. A.C.O. and G.V. were supported by the Max Planck Society, the European Research Council (ERC) under the European Communities 7th Framework Programme [FP7/2007–2013]/[ERC grant 207634], the Wellcome Trust [WT098025MA] and the Medical Research Council [MC_UP_1202/3], and G.V. by an EMBO long-term fellowship [ALTF 1572-2011]. F.C.W. and A.C.N. were supported by a Lister Institute for Preventive Medicine Research Prize. H.T. was supported by an A*STAR Graduate Academy scholarship. Deposited in PMC for release after 12 months.

Supplementary material

Supplementary material available online at
http://dev.biologists.org/lookup/suppl/doi:10.1242/dev.113431/-/DC1

References

Akiyama, R., Masuda, M., Tsuge, S., Bessho, Y. and Matsui, T. (2014). An anterior limit of FGF/Erk signal activity marks the earliest future somite boundary in zebrafish. *Development* **141**, 1104-1109.

Aulehla, A. and Pourquié, O. (2010). Signaling gradients during paraxial mesoderm development. *Cold Spring Harb. Perspect. Biol.* **2**, a000869.

Barresi, M. J., Stickney, H. L. and Devoto, S. H. (2000). The zebrafish slow-muscle-omitted gene product is required for Hedgehog signal transduction and the development of slow muscle identity. *Development* **127**, 2189-2199.

Blagden, C. S., Currie, P. D., Ingham, P. W. and Hughes, S. M. (1997). Notochord induction of zebrafish slow muscle mediated by Sonic hedgehog. *Genes Dev.* **11**, 2163-2175.

Bondue, A., Lapouge, G., Paulissen, C., Semeraro, C., Iacovino, M., Kyba, M. and Blanpain, C. (2008). Mesp1 acts as a master regulator of multipotent cardiovascular progenitor specification. *Cell Stem Cell* **3**, 69-84.

Brend, T. and Holley, S. A. (2009). Expression of the oscillating gene her1 is directly regulated by hairy/enhancer of split, T-box, and suppressor of Hairless proteins in the zebrafish segmentation clock. *Dev. Dyn.* **238**, 2745-2759.

Buckingham, M. and Relaix, F. (2007). The role of Pax genes in the development of tissues and organs: Pax3 and Pax7 regulate muscle progenitor cell functions. *Annu. Rev. Cell Dev. Biol.* **23**, 645-673.

Buckingham, M. and Rigby, P. W. J. (2014). Gene regulatory networks and transcriptional mechanisms that control myogenesis. *Dev. Cell* **28**, 225-238.

Buckingham, M. and Vincent, S. D. (2009). Distinct and dynamic myogenic populations in the vertebrate embryo. *Curr. Opin. Genet. Dev.* **19**, 444-453.

Cutty, S. J., Fior, R., Henriques, P. M., Saúde, L. and Wardle, F. C. (2012). Identification and expression analysis of two novel members of the Mesp family in zebrafish. *Int. J. Dev. Biol.* **56**, 285-294.

Dahmann, C., Oates, A. C. and Brand, M. (2011). Boundary formation and maintenance in tissue development. *Nat. Rev. Genet.* **12**, 43-55.

Devoto, S. H., Stoiber, W., Hammond, C. L., Steinbacher, P., Haslett, J. R., Barresi, M. J. F., Patterson, S. E., Adiarte, E. G. and Hughes, S. M. (2006).

Generality of vertebrate developmental patterns: evidence for a dermomyotome in fish. *Evol. Dev.* **8**, 101-110.
Du, S. J., Devoto, S. H., Westerfield, M. and Moon, R. T. (1997). Positive and negative regulation of muscle cell identity by members of the hedgehog and TGF-beta gene families. *J. Cell Biol.* **139**, 145-156.
Dubrulle, J., McGrew, M. J. and Pourquié, O. (2001). FGF signaling controls somite boundary position and regulates segmentation clock control of spatiotemporal Hox gene activation. *Cell* **106**, 219-232.
Garnett, A. T., Han, T. M., Gilchrist, M. J., Smith, J. C., Eisen, M. B., Wardle, F. C. and Amacher, S. L. (2009). Identification of direct T-box target genes in the developing zebrafish mesoderm. *Development* **136**, 749-760.
Groves, J. A., Hammond, C. L. and Hughes, S. M. (2005). Fgf8 drives myogenic progression of a novel lateral fast muscle fibre population in zebrafish. *Development* **132**, 4211-4222.
Hammond, C. L., Hinits, Y., Osborn, D. P. S., Minchin, J. E. N., Tettamanti, G. and Hughes, S. M. (2007). Signals and myogenic regulatory factors restrict pax3 and pax7 expression to dermomyotome-like tissue in zebrafish. *Dev. Biol.* **302**, 504-521.
Holley, S. A. (2007). The genetics and embryology of zebrafish metamerism. *Dev. Dyn.* **236**, 1422-1449.
Hollway, G. E., Bryson-Richardson, R. J., Berger, S., Cole, N. J., Hall, T. E. and Currie, P. D. (2007). Whole-somite rotation generates muscle progenitor cell compartments in the developing zebrafish embryo. *Dev. Cell* **12**, 207-219.
Kawamura, A., Koshida, S., Hijikata, H., Ohbayashi, A., Kondoh, H. and Takada, S. (2005). Groucho-associated transcriptional repressor ripply1 is required for proper transition from the presomitic mesoderm to somites. *Dev. Cell* **9**, 735-744.
Kawamura, A., Koshida, S. and Takada, S. (2008). Activator-to-repressor conversion of T-box transcription factors by the Ripply family of Groucho/TLE-associated mediators. *Mol. Cell. Biol.* **28**, 3236-3244.
Kispert, A. and Hermann, B. G. (1993). The Brachyury gene encodes a novel DNA binding protein. *EMBO J.* **12**, 4898-4899.
Kondow, A., Hitachi, K., Okabayashi, K., Hayashi, N. and Asashima, M. (2007). Bowline mediates association of the transcriptional corepressor XGrg-4 with Tbx6 during somitogenesis in Xenopus. *Biochem. Biophys. Res. Commun.* **359**, 959-964.
Kusakabe, R. and Kuratani, S. (2005). Evolution and developmental patterning of the vertebrate skeletal muscles: perspectives from the lamprey. *Dev. Dyn.* **234**, 824-834.
Kwan, K. M., Fujimoto, E., Grabher, C., Mangum, B. D., Hardy, M. E., Campbell, D. S., Parant, J. M., Yost, H. J., Kanki, J. P. and Chien, C.-B. (2007). The Tol2kit: a multisite gateway-based construction kit for Tol2 transposon transgenesis constructs. *Dev. Dyn.* **236**, 3088-3099.
Langmead, B., Trapnell, C., Pop, M. and Salzberg, S. L. (2009). Ultrafast and memory-efficient alignment of short DNA sequences to the human genome. *Genome Biol.* **10**, R25.
Lenhard, B. and Wasserman, W. W. (2002). TFBS: computational framework for transcription factor binding site analysis. *Bioinformatics* **18**, 1135-1136.
Mankoo, B. S., Skuntz, S., Harrigan, I., Grigorieva, E., Candia, A., Wright, C. V. E., Arnheiter, H. and Pachnis, V. (2003). The concerted action of Meox homeobox genes is required upstream of genetic pathways essential for the formation, patterning and differentiation of somites. *Development* **130**, 4655-4664.
Moreno, T. A., Jappelli, R., Izpisua Belmonte, J. C. and Kintner, C. (2008). Retinoic acid regulation of the Mesp-Ripply feedback loop during vertebrate segmental patterning. *Dev. Biol.* **315**, 317-330.
Morimoto, M., Sasaki, N., Oginuma, M., Kiso, M., Igarashi, K., Aizaki, K.-i., Kanno, J. and Saga, Y. (2007). The negative regulation of Mesp2 by mouse Ripply2 is required to establish the rostro-caudal patterning within a somite. *Development* **134**, 1561-1569.
Nakajima, Y., Morimoto, M., Takahashi, Y., Koseki, H. and Saga, Y. (2006). Identification of Epha4 enhancer required for segmental expression and the regulation by Mesp2. *Development* **133**, 2517-2525.
Nikaido, M., Kawakami, A., Sawada, A., Furutani-Seiki, M., Takeda, H. and Araki, K. (2002). Tbx24, encoding a T-box protein, is mutated in the zebrafish somite-segmentation mutant fused somites. *Nat. Genet.* **31**, 195-199.
Oates, A. C., Rohde, L. A. and Ho, R. K. (2005). Generation of segment polarity in the paraxial mesoderm of the zebrafish through a T-box-dependent inductive event. *Dev. Biol.* **283**, 204-214.
Oates, A. C., Morelli, L. G. and Ares, S. (2012). Patterning embryos with oscillations: structure, function and dynamics of the vertebrate segmentation clock. *Development* **139**, 625-639.
Oginuma, M., Hirata, T. and Saga, Y. (2008). Identification of presomitic mesoderm (PSM)-specific Mesp1 enhancer and generation of a PSM-specific Mesp1/Mesp2-null mouse using BAC-based rescue technology. *Mech. Dev.* **125**, 432-440.
Patterson, S. E., Bird, N. C. and Devoto, S. H. (2010). BMP regulation of myogenesis in zebrafish. *Dev. Dyn.* **239**, 806-817.
Pavesi, G., Mereghetti, P., Zambelli, F., Stefani, M., Mauri, G. and Pesole, G. (2006). MoD Tools: regulatory motif discovery in nucleotide sequences from co-regulated or homologous genes. *Nucleic Acids Res.* **34**, W566-W570.
Pourquié, O. (2011). Vertebrate segmentation: from cyclic gene networks to scoliosis. *Cell* **145**, 650-663.
Saga, Y. (2012). The mechanism of somite formation in mice. *Curr. Opin. Genet. Dev.* **22**, 331-338.
Saga, Y., Hata, N., Koseki, H. and Taketo, M. M. (1997). Mesp2: a novel mouse gene expressed in the presegmented mesoderm and essential for segmentation initiation. *Genes Dev.* **11**, 1827-1839.
Sawada, A., Fritz, A., Jiang, Y. J., Yamamoto, A., Yamasu, K., Kuroiwa, A., Saga, Y. and Takeda, H. (2000). Zebrafish Mesp family genes, mesp-a and mesp-b are segmentally expressed in the presomitic mesoderm, and Mesp-b confers the anterior identity to the developing somites. *Development* **127**, 1691-1702.
Stellabotte, F., Dobbs-McAuliffe, B., Fernandez, D. A., Feng, X. and Devoto, S. H. (2007). Dynamic somite cell rearrangements lead to distinct waves of myotome growth. *Development* **134**, 1253-1257.
Stellabotte, F. and Devoto, S. H. (2007). The teleost dermomyotome. *Dev. Dyn.* **236**, 2432-2443.
Takahashi, Y., Hiraoka, S., Kitajima, S., Inoue, T., Kanno, J. and Saga, Y. (2005). Differential contributions of Mesp1 and Mesp2 to the epithelialization and rostro-caudal patterning of somites. *Development* **132**, 787-796.
Takahashi, J., Ohbayashi, A., Oginuma, M., Saito, D., Mochizuki, A., Saga, Y. and Takada, S. (2010). Analysis of Ripply1/2-deficient mouse embryos reveals a mechanism underlying the rostro-caudal patterning within a somite. *Dev. Biol.* **342**, 134-145.
Tazumi, S., Yabe, S., Yokoyama, J., Aihara, Y. and Uchiyama, H. (2008). pMesogenin1 and 2 function directly downstream of Xtbx6 in Xenopus somitogenesis and myogenesis. *Dev. Dyn.* **237**, 3749-3761.
Terasaki, H., Murakami, R., Yasuhiko, Y., Shin, I. T., Kohara, Y., Saga, Y. and Takeda, H. (2006). Transgenic analysis of the medaka mesp-b enhancer in somitogenesis. *Dev. Growth Differ.* **48**, 153-168.
van Eeden, F. J., Granato, M., Schach, U., Brand, M., Furutani-Seiki, M., Haffter, P., Hammerschmidt, M., Heisenberg, C. P., Jiang, Y. J., Kane, D. A. et al. (1996). Mutations affecting somite formation and patterning in the zebrafish, Danio rerio. *Development* **123**, 153-164.
Villefranc, J. A., Amigo, J. and Lawson, N. D. (2007). Gateway compatible vectors for analysis of gene function in the zebrafish. *Dev. Dyn.* **236**, 3077-3087.
Wardle, F. C., Odom, D. T., Bell, G. W., Yuan, B., Danford, T. W., Wiellette, E. L., Herbolsheimer, E., Sive, H. L., Young, R. A. and Smith, J. C. (2006). Zebrafish promoter microarrays identify actively transcribed embryonic genes. *Genome Biol.* **7**, R71.
Westerfield, M. (1995). *The Zebrafish Book*, 3rd ed. Eugene, Oregon, University of Oregon Press.
Windner, S. E., Bird, N. C., Patterson, S. E., Doris, R. A. and Devoto, S. H. (2012). Fss/Tbx6 is required for central dermomyotome cell fate in zebrafish. *Biol. Open* **1**, 806-814.
Yasuhiko, Y., Haraguchi, S., Kitajima, S., Takahashi, Y., Kanno, J. and Saga, Y. (2006). Tbx6-mediated Notch signaling controls somite-specific Mesp2 expression. *Proc. Natl. Acad. Sci. USA* **103**, 3651-3656.
Yasuhiko, Y., Kitajima, S., Takahashi, Y., Oginuma, M., Kagiwada, H., Kanno, J. and Saga, Y. (2008). Functional importance of evolutionally conserved Tbx6 binding sites in the presomitic mesoderm-specific enhancer of Mesp2. *Development* **135**, 3511-3519.
Zhang, Y., Liu, T., Meyer, C. A., Eeckhoute, J., Johnson, D. S., Bernstein, B. E., Nusbaum, C., Myers, R. M., Brown, M., Li, W. et al. (2008). Model-based analysis of ChIP-Seq (MACS). *Genome Biol.* **9**, R137.

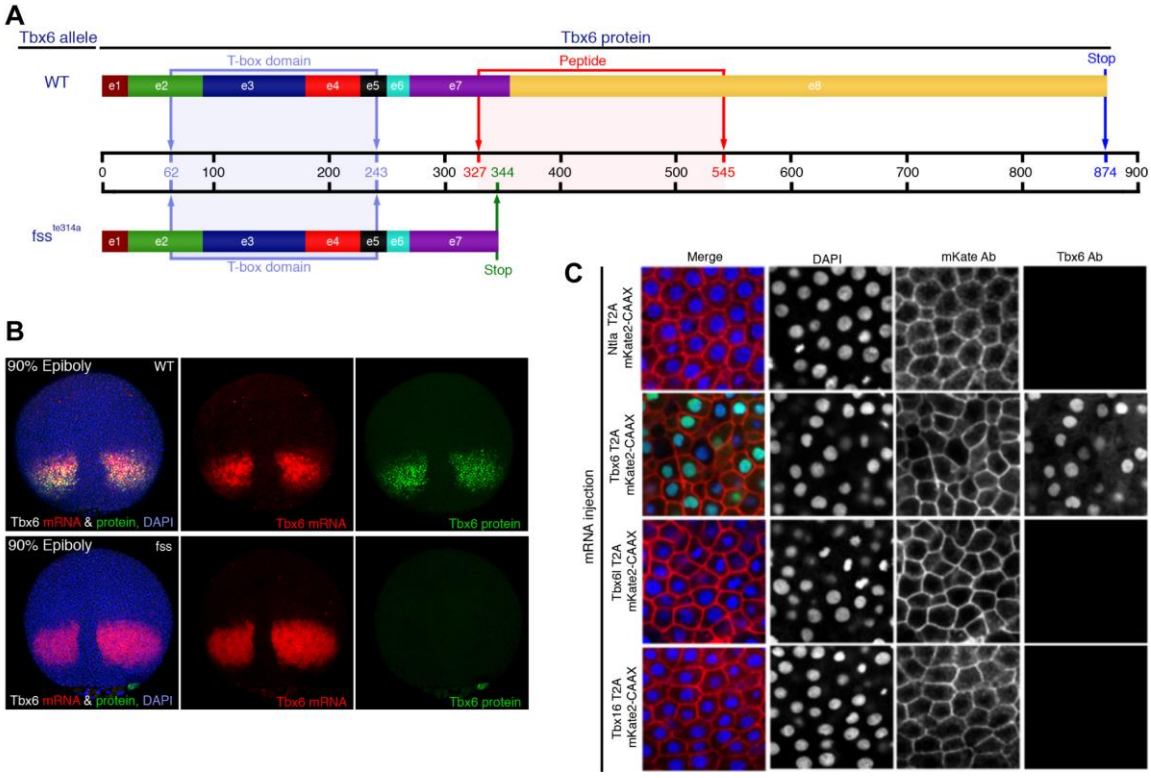

Figure S1. Tbx6 antibody-binding specificity. (A) Graphical representation of the full-length Tbx6 protein in wild-type embryos, and the truncated Tbx6 protein in *tbx6* mutants. All eight exons are depicted in different colors. The blue arrows represent the predicted T-box domain from amino acid 62 to 243. The sequence chosen to generate the Tbx6 antibody is highlighted in red, spanning the region from amino acid 327 to 545. (B) Representative example showing *tbx6* mRNA and protein expression patterns in wild type and in *tbx6* mutants at 90% epiboly. Immunolabeling using the Tbx6 antibody was followed by *in situ* hybridization using a *tbx6* probe and the Fast Red reaction (Roche) (C) Immunolabeling using Tbx6 (green) and tRFP (red fluorescent protein mKate2) antibodies. Animal poles of *tbx6* mutant embryos 4 hours post fertilization, injected at the 1-cell-stage with capped mRNAs (generated using the Tol2 kit and the mMessage kit, Ambion): *Ntla-T2A-mKate2CAAX*, *Tbx6-T2A-mKate2CAAX*, *Tbx6l-T2A-mKate2CAAX* or *Tbx16-T2A-mKate2CAAX*. The Tbx6 antibody only binds in embryos injected with *tbx6* mRNA. Embryos were imaged with a Zeiss LSM 780 and confocal *z*-stacks were flattened.

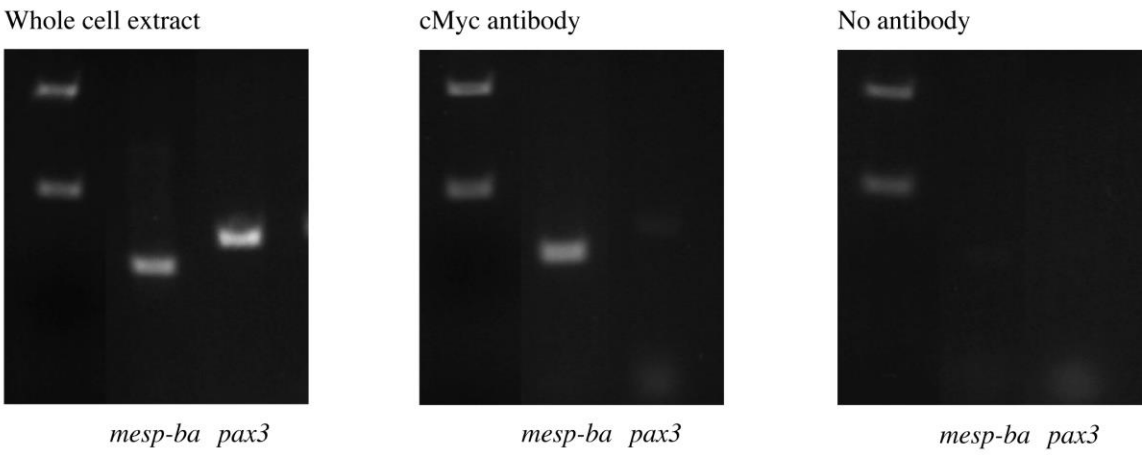

Figure S2. ChIP-PCR confirming Tbx6^{Myc} binding approximately 6700 bp upstream of the *mesp-ba* transcriptional start site (peak 16075430-16075735). *Tg(hsp70l:tbx6^{myc})* and wild-type embryos were heat-shocked, fixed and extracted as for ChIP-Seq. The extract was immunoprecipitated using the Myc epitope antibody (9B11, Cell Signaling Technology), as in Martins-Taylor et al. (2011). The DNA isolated by ChIP was amplified using the following primers: *mesp-ba* 5'-AATGGTAGTCAGGCAGAAGTG-3', 5'-CTGCAGCAAGTTGCCTTACAG-3'; *pax3* 5'-AGTAGTATCGCCCGGTCTTCTC-3', 5,-CCTGAGGGACAAAACATC-3'. Specificity of Tbx6^{Myc} binding was confirmed, as DNA upstream of the *pax3* gene is not pulled down using a Myc antibody, serving as a negative control, whereas a no-Myc-antibody control fails to immunoprecipitate DNA from upstream both of *mesp-ba* and *pax3*. Peak 16082055-16082560 was confirmed by Kawamura et al. (2008), using the following primers: 5'-CAACAAACACAAAAAGCACACGTT-3', 5'-GGTGAAAGGAGGATGGAGGTTTAT-3'.

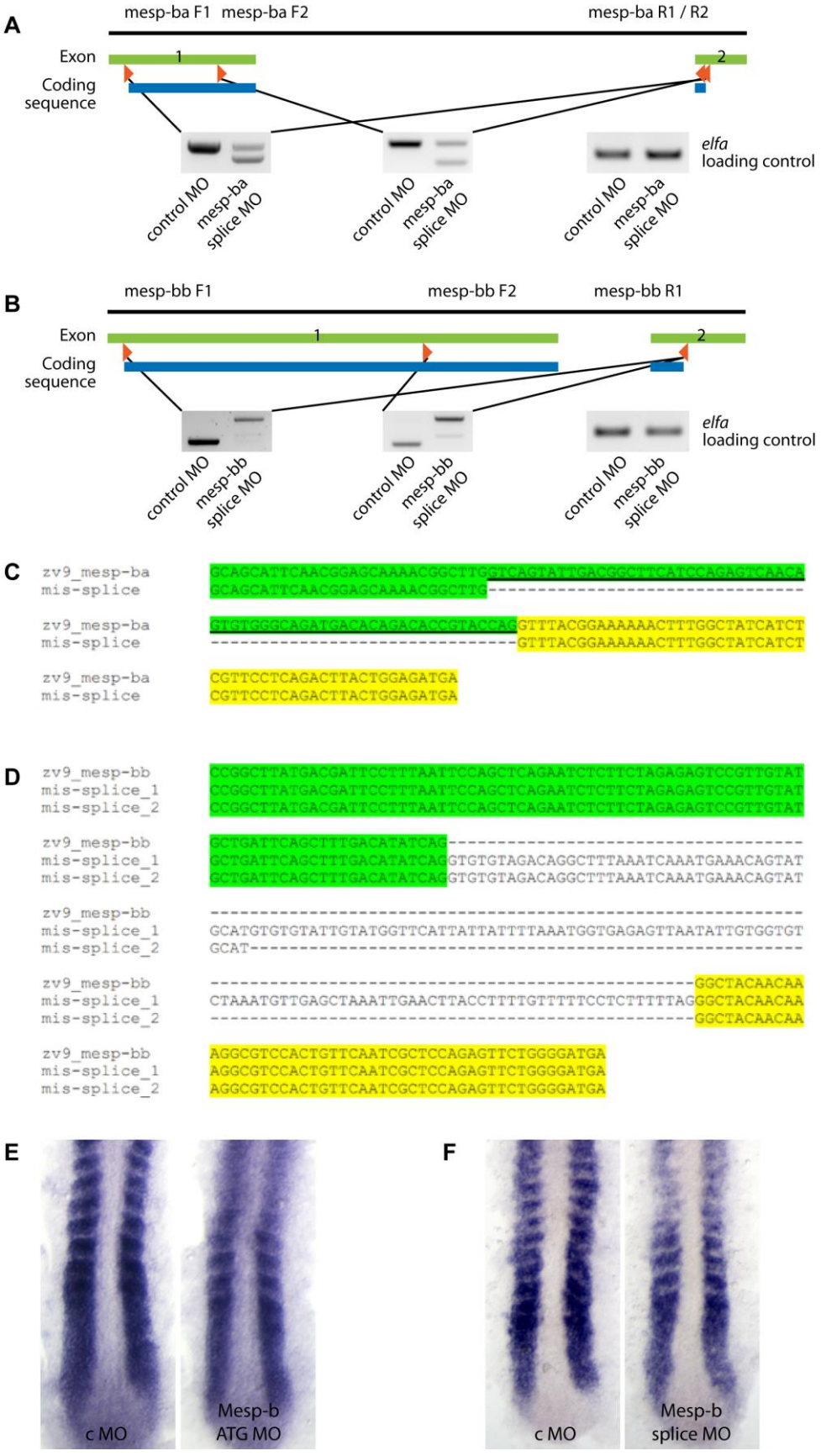

Figure S3. Mesp-b MO validation. (A,B) Mesp-ba (A) and Mesp-bb (B) splice morpholino transcript schematics and PCR primers are shown on top, the RT-PCR of

injected embryos is shown below. (C) Green highlight - 3' part of Zv9 *mesp-ba* exon 1; Yellow highlight - Zv9 *mesp-ba* exon 2 (until stop codon, excluding 3' UTR); Underlined - Sequence missing from *mesp-ba* mis-splice product. (D) Green highlight - 3' part of Zv9 *mesp-bb* exon 1; Yellow highlight - Zv9 *mesp-bb* exon 2 (until stop codon, excluding 3' UTR). Mis-splice_1 is the larger product, mis-splice_2 the smaller product shown in (B). (E,F) In situ hybridization for *meox1* mRNA in control and Mesp-b MO-treated embryos. Mesp-b ATG MOs and Mesp-b splice MOs cause similar reduction of *meox1* expression in maturing somites.

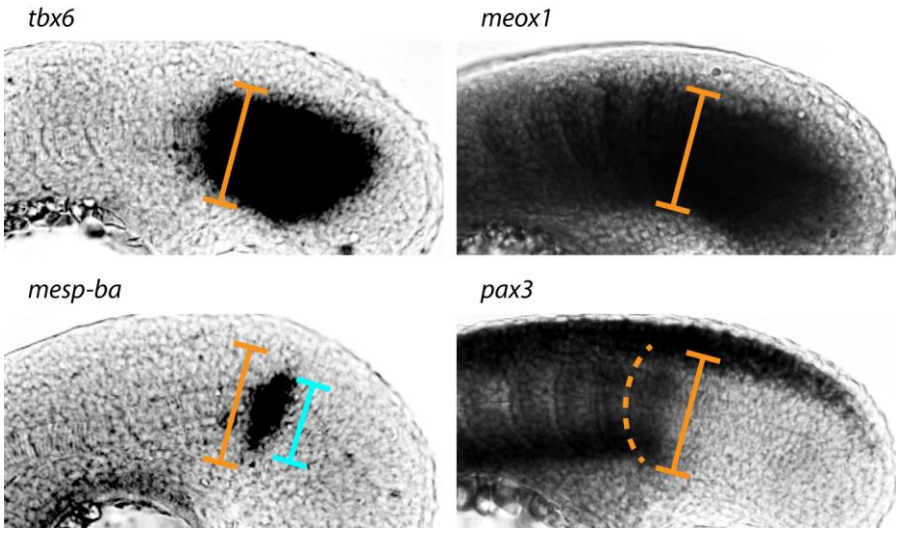

Figure S4. Expression of *tbx6, meox1, mesp-ba* and *pax3* mRNA. Expression of *tbx6*, *meox1* and *pax3* spans the entire dorsal-ventral extent of the paraxial mesoderm (orange brackets). *mesp-ba* mRNA is highly expressed in the central region (blue bracket) but not detectable in the peripheral portions of the presomitic paraxial mesoderm. Dashed line indicates most recently formed somite boundary.

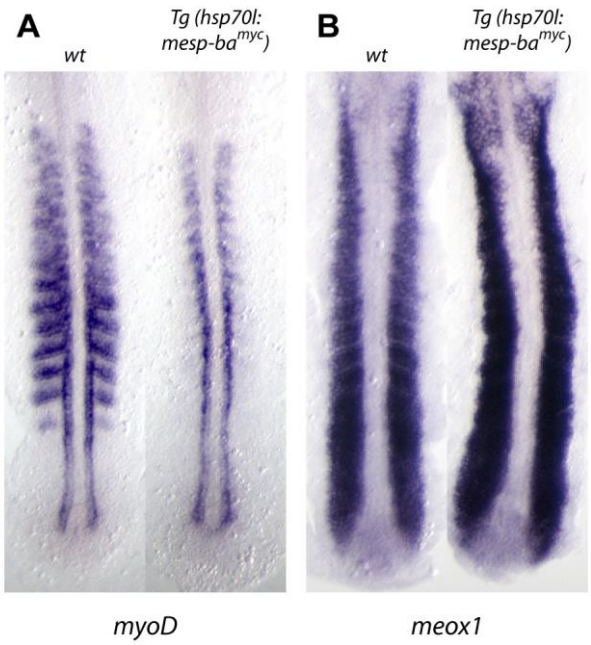

Figure S5. Ubiquitous Mesp-ba expression immediately changes *myoD* and *meox1* mRNA levels. *In situ* hybridization for *myoD* (C) and *meox1* (D) in wild-type (left side) and *Tg(hsp70l:mesp-ba^{myc})* embryos (right side) 15 minutes after the end of a 1-h heat shock. *myoD* is downregulated and *meox1* is upregulated in the lateral paraxial mesoderm.

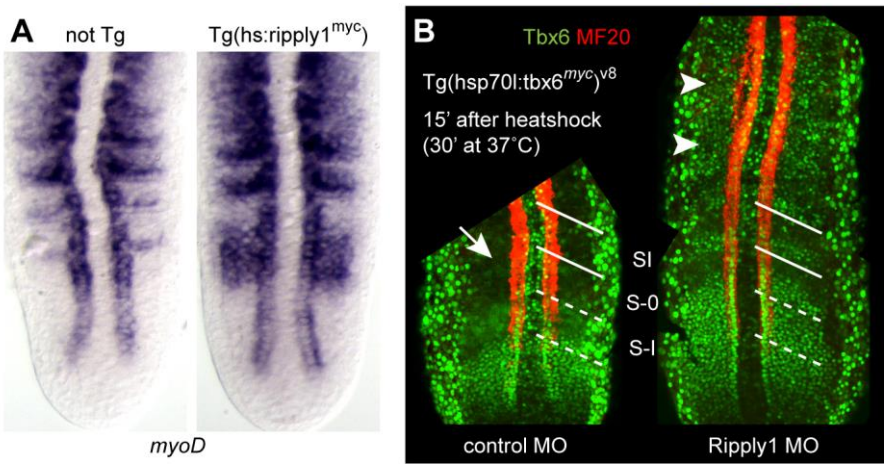

Figure S6. Ripply1 regulates Tbx6 function. (A) *In situ* hybridization for *myoD* in wild-type embryos and *Tg(hsp70l:ripply1^{myc})* siblings after a series of three heat shocks (30 minutes each, followed by 30-minute breaks). Ubiquitous expression of Ripply1 leads to an increase of *myoD* expression in the anterior presomitic mesoderm. (B) *Tg(hsp70l:tbx6^{myc})^{v8}* embryos, injected with control (left) or Ripply1 MOs (right); heat-shocked at the 10S stage for 30 minutes and fixed 15 minutes after the end of heatshock treatment. Immunolabeling shows expression of Tbx6 (green) and myosin heavy chain (MF20, red). Immediately after ubiquitous Tbx6^{Myc} expression, Tbx6 protein is cleared from the paraxial mesoderm in control but not in Ripply1 MO-treated embryos.

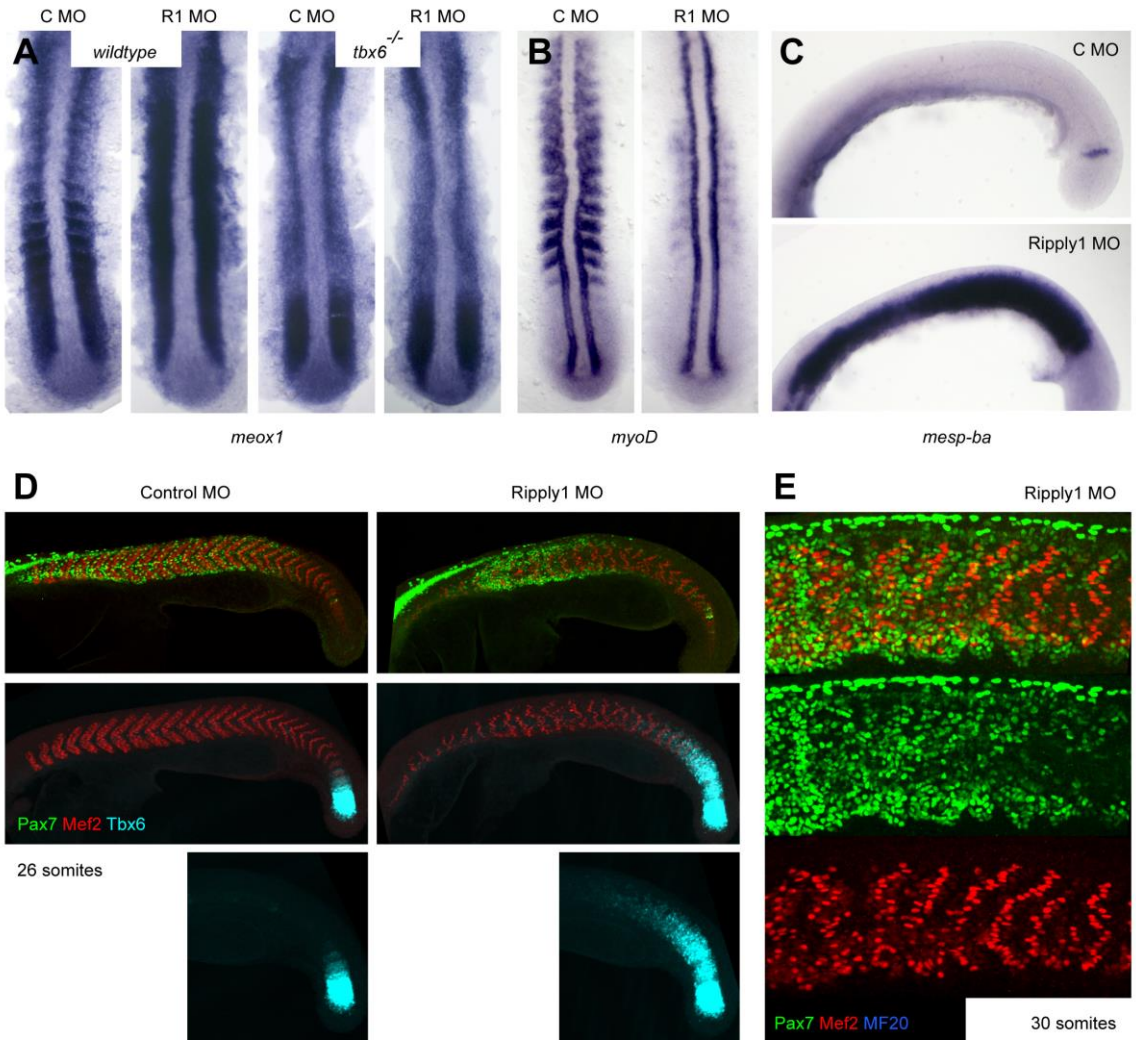

Figure S7. Knockdown of Ripply1 promotes dermomyotome development at the expense of primary fast myotome primary fast muscle formation but delays maturation. (A-C) *In situ* hybridization for *meox1* (A), *myoD* (B) and *mesp-ba* (C) in control MO and Ripply1 MO-injected embryos during segmentation. Note that Ripply1 MO treatment shows no effects in *tbx6* mutants. (D,E) Immunolabeling in Ripply1 MO- and control MO-treated embryos. (D) Comparison of Pax7 (green) and Tbx6 expression (cyan) in embryos at the 26S stage. Myonuclei are labeled with Mef2 (red). (E) Ripply1 morphant showing that the onset of Pax7 expression (green) spatially correlates with the appearance of the first primary fast myotome cells (Mef2, faint red). Slow fiber nuclei express Mef2 (bright) before the maturation of the dermomyotome.

Table S1. ChIP-Seq. Tables listing the positions of significant peaks identified in duplicate anti-Myc immunoprecipitation experiments from *Tg(hsp70l:tbx6^{myc})* embryos 1 h after heat shock treatment (see Fig. 1F), and corresponding gene positions.

Chromosome	Peak start	Peak stop	Peak size	Proximal gene
chr7	16074838	16075110	273	*mespba;mespaa*
chr7	**16075430**	**16075735**	306	*mespba;mespaa*
chr7	16077395	16077604	210	*mespba;mespaa*
chr7	**16082055**	**16082560**	506	*mespaa;mespba*
chr21	36933621	36934092	472	*mespbb;mespab*
chr21	36935687	36936177	491	*mespbb;mespab*
chr21	36936989	36937357	369	*mespbb;mespab*
chr21	36951345	36951918	574	*mespbb;mespab*
chr21	36952555	36952924	370	*mespbb;mespab*
chr21	36958013	36958556	544	*mespbb;mespab*
chr21	36960812	36961218	407	*mespbb;mespab*
chr25	11386856	11387147	292	*ripply1*
chr25	11386856	11387147	292	*ripply1*
chr25	11389407	11389883	477	*ripply1*
chr25	11393143	11393773	631	*ripply1*
chr25	11396259	11396835	577	*ripply1*
chr25	11398508	11398877	370	*ripply1*
chr25	11400599	11401158	560	*ripply1*

Gene name	Chromosome	Gene start	Gene stop	Strand
mespaa	chr7	16098653	16101163	1
mespba	chr7	16082277	16085567	1
mespab	chr25	11382068	11383326	-1
mespbb	chr25	11392554	11393558	-1
ripply1	chr21	36930713	36937075	-1

Table S2. Location of potential T-boxes within genomic regions represented in Figure 1F.

All Tboxes of >50% of the maximum possible score relative to the motif identified in this study are shown (see Materials and Methods). Whether each sequence is located under a ChIP-seq peak is indicated.

Chromosome	Region start	Region end	Tbox start	Tbox end	Tbox strand	% of max. score	Sequence	Under ChIP-seq peak
7	16069000	16104000	16070479	16070486	+	59.2	TCACACAC	
7	16069000	16104000	16070660	16070667	-	54.8	TCACAGCA	
7	16069000	16104000	16071406	16071413	-	54.8	TCACAGCA	
7	16069000	16104000	16071516	16071523	-	61.5	TCACACTA	
7	16069000	16104000	16071869	16071876	-	83.3	TCACACTT	
7	16069000	16104000	16072717	16072724	-	57.3	TGACACCA	
7	16069000	16104000	16074474	16074481	+	54.8	TCACAGCA	
7	16069000	16104000	16075011	16075018	+	100.0	TCACACCT	*
7	16069000	16104000	16075046	16075053	-	100.0	TCACACCT	*
7	16069000	16104000	16075312	16075319	-	100.0	TCACACCT	
7	16069000	16104000	16075592	16075599	+	61.5	TCACACTA	*
7	16069000	16104000	16077272	16077279	-	72.0	TCACATCT	
7	16069000	16104000	16077486	16077493	-	59.0	TCACACAA	*
7	16069000	16104000	16077497	16077504	+	100.0	TCACACCT	*
7	16069000	16104000	16077744	16077751	-	55.4	TCACATTT	
7	16069000	16104000	16078528	16078535	+	60.5	ACACACTT	
7	16069000	16104000	16078566	16078573	+	56.4	AGACACCT	
7	16069000	16104000	16078600	16078607	+	58.1	ACACACAT	
7	16069000	16104000	16078629	16078636	+	58.1	ACACACAT	
7	16069000	16104000	16079062	16079069	-	60.0	TCACAGTT	
7	16069000	16104000	16079666	16079673	+	83.3	TCACACTT	
7	16069000	16104000	16080777	16080784	+	55.4	TCACATTT	
7	16069000	16104000	16082207	16082214	+	100.0	TCACACCT	*
7	16069000	16104000	16082307	16082314	-	79.2	TGACACCT	*
7	16069000	16104000	16082310	16082317	+	55.2	TGTCACCT	*
7	16069000	16104000	16082740	16082747	+	52.6	TCTCAGCT	
7	16069000	16104000	16083275	16083282	+	55.3	ACACACCA	
7	16069000	16104000	16083386	16083393	-	60.1	TGACACAT	
7	16069000	16104000	16084350	16084357	-	58.1	ACACACAT	
7	16069000	16104000	16084624	16084631	+	55.4	TCACATTT	
7	16069000	16104000	16084808	16084815	-	79.2	TGACACCT	
7	16069000	16104000	16084871	16084878	+	77.2	ACACACCT	
7	16069000	16104000	16084924	16084931	-	60.5	ACACACTT	
7	16069000	16104000	16085135	16085142	+	51.3	TGACATCT	

7	16069000	16104000	16085366	16085373	+	78.1	TCACACCA	
7	16069000	16104000	16086360	16086367	-	76.7	TCACAGCT	
7	16069000	16104000	16088251	16088258	+	83.3	TCACACTT	
7	16069000	16104000	16089113	16089120	+	80.9	TCACACAT	
7	16069000	16104000	16089181	16089188	-	52.9	TCACATAT	
7	16069000	16104000	16089327	16089334	+	77.2	ACACACCT	
7	16069000	16104000	16089937	16089944	-	72.0	TCACATCT	
7	16069000	16104000	16090015	16090022	+	78.1	TCACACCA	
7	16069000	16104000	16090098	16090105	-	53.9	ACACAGCT	
7	16069000	16104000	16090220	16090227	+	58.1	ACACACAT	
7	16069000	16104000	16090266	16090273	-	80.9	TCACACAT	
7	16069000	16104000	16091463	16091470	+	58.1	ACACACAT	
7	16069000	16104000	16091896	16091903	+	80.9	TCACACAT	
7	16069000	16104000	16092292	16092299	+	80.9	TCACACAT	
7	16069000	16104000	16092376	16092383	-	83.3	TCACACTT	
7	16069000	16104000	16092567	16092574	+	52.9	TCACATAT	
7	16069000	16104000	16093663	16093670	+	100.0	TCACACCT	
7	16069000	16104000	16093721	16093728	+	51.3	TGACATCT	
7	16069000	16104000	16093753	16093760	+	57.3	TGACACCA	
7	16069000	16104000	16094026	16094033	-	78.3	TCACACCC	
7	16069000	16104000	16094395	16094402	+	55.3	ACACACCA	
7	16069000	16104000	16094402	16094409	-	55.4	TCACATTT	
7	16069000	16104000	16095140	16095147	-	53.9	ACACAGCT	
7	16069000	16104000	16095370	16095377	+	55.3	ACACACCA	
7	16069000	16104000	16095782	16095789	+	55.9	TGACAGCT	
7	16069000	16104000	16096636	16096643	+	60.5	ACACACTT	
7	16069000	16104000	16098455	16098462	-	80.9	TCACACAT	
7	16069000	16104000	16098493	16098500	+	100.0	TCACACCT	
7	16069000	16104000	16098980	16098987	+	54.1	TCTCACCA	
7	16069000	16104000	16099252	16099259	-	77.2	ACACACCT	
7	16069000	16104000	16099403	16099410	-	77.2	ACACACCT	
7	16069000	16104000	16099559	16099566	-	77.2	ACACACCT	
7	16069000	16104000	16099658	16099665	-	77.2	ACACACCT	
7	16069000	16104000	16100250	16100257	+	80.9	TCACACAT	
7	16069000	16104000	16101249	16101256	+	58.1	ACACACAT	
7	16069000	16104000	16101319	16101326	+	55.4	TCACATTT	
7	16069000	16104000	16102155	16102162	+	83.3	TCACACTT	
7	16069000	16104000	16102503	16102510	+	62.5	TGACACTT	
7	16069000	16104000	16102881	16102888	-	100.0	TCACACCT	
7	16069000	16104000	16103051	16103058	-	75.9	TCTCACCT	
7	16069000	16104000	16103084	16103091	+	53.9	ACACAGCT	
21	36929000	36964000	36929777	36929784	+	53.9	ACACAGCT	
21	36929000	36964000	36930193	36930200	-	55.4	TCACATTT	
21	36929000	36964000	36930258	36930265	+	56.4	AGACACCT	

21	36929000	36964000	36930669	36930676	-	83.3	TCACACTT	
21	36929000	36964000	36930680	36930687	-	55.2	TGTCACCT	
21	36929000	36964000	36931149	36931156	-	76.7	TCACAGCT	
21	36929000	36964000	36931207	36931214	+	76.7	TCACAGCT	
21	36929000	36964000	36931821	36931828	+	60.5	ACACACTT	
21	36929000	36964000	36933115	36933122	-	58.1	ACACACAT	
21	36929000	36964000	36933794	36933801	-	76.7	TCACAGCT	*
21	36929000	36964000	36933809	36933816	-	57.5	TGACACCC	*
21	36929000	36964000	36933865	36933872	-	56.4	AGACACCT	*
21	36929000	36964000	36933892	36933899	-	52.6	TCTCAGCT	*
21	36929000	36964000	36933942	36933949	+	61.7	TCACACTC	*
21	36929000	36964000	36934043	36934050	+	55.2	TGTCACCT	*
21	36929000	36964000	36934098	36934105	+	59.2	TCACACAC	
21	36929000	36964000	36934102	36934109	+	53.9	ACACAGCT	
21	36929000	36964000	36935434	36935441	+	59.0	TCACACAA	
21	36929000	36964000	36935595	36935602	+	53.2	ACTCACCT	
21	36929000	36964000	36935961	36935968	-	54.3	TCTCACCC	*
21	36929000	36964000	36936350	36936357	-	60.5	ACACACTT	
21	36929000	36964000	36937790	36937797	-	59.2	TCACACAC	
21	36929000	36964000	36937865	36937872	+	76.7	TCACAGCT	
21	36929000	36964000	36938150	36938157	-	80.9	TCACACAT	
21	36929000	36964000	36938997	36939004	-	55.4	TCACATTT	
21	36929000	36964000	36939117	36939124	+	54.8	TCACAGCA	
21	36929000	36964000	36939198	36939205	+	56.8	TCTCACAT	
21	36929000	36964000	36939200	36939207	+	72.0	TCACATCT	
21	36929000	36964000	36939244	36939251	-	59.3	TCTCACTT	
21	36929000	36964000	36939778	36939785	-	54.8	TCACAGCA	
21	36929000	36964000	36940197	36940204	-	53.2	ACTCACCT	
21	36929000	36964000	36940461	36940468	-	54.3	TCTCACCC	
21	36929000	36964000	36941676	36941683	-	100.0	TCACACCT	
21	36929000	36964000	36942141	36942148	+	50.2	TCACATCA	
21	36929000	36964000	36942463	36942470	-	53.9	ACACAGCT	
21	36929000	36964000	36942743	36942750	+	59.0	TCACACAA	
21	36929000	36964000	36942871	36942878	-	83.3	TCACACTT	
21	36929000	36964000	36942925	36942932	+	78.1	TCACACCA	
21	36929000	36964000	36943284	36943291	+	57.3	TGACACCA	
21	36929000	36964000	36944187	36944194	+	59.3	TCTCACTT	
21	36929000	36964000	36944209	36944216	+	50.2	TCACATCA	
21	36929000	36964000	36944228	36944235	-	77.2	ACACACCT	
21	36929000	36964000	36944621	36944628	-	57.5	TGACACCC	
21	36929000	36964000	36944796	36944803	-	59.0	TCACACAA	
21	36929000	36964000	36944990	36944997	+	59.0	TCACACAA	
21	36929000	36964000	36945026	36945033	+	57.5	TCACAGAT	
21	36929000	36964000	36945206	36945213	-	53.9	ACACAGCT	

21	36929000	36964000	36945410	36945417	+	59.3	TCTCACTT	
21	36929000	36964000	36945450	36945457	-	77.2	ACACACCT	
21	36929000	36964000	36945454	36945461	-	59.2	TCACACAC	
21	36929000	36964000	36945461	36945468	+	56.4	AGACACCT	
21	36929000	36964000	36946596	36946603	+	72.0	TCACATCT	
21	36929000	36964000	36947037	36947044	+	59.2	TCACACAC	
21	36929000	36964000	36947500	36947507	+	77.2	ACACACCT	
21	36929000	36964000	36947552	36947559	-	77.2	ACACACCT	
21	36929000	36964000	36947567	36947574	-	54.3	TCTCACCC	
21	36929000	36964000	36947574	36947581	-	53.9	ACACAGCT	
21	36929000	36964000	36948050	36948057	+	61.5	TCACACTA	
21	36929000	36964000	36948126	36948133	+	50.2	TCACATCA	
21	36929000	36964000	36948548	36948555	+	61.5	TCACACTA	
21	36929000	36964000	36948712	36948719	-	61.5	TCACACTA	
21	36929000	36964000	36948837	36948844	+	61.7	TCACACTC	
21	36929000	36964000	36948971	36948978	-	77.2	ACACACCT	
21	36929000	36964000	36949300	36949307	+	58.1	ACACACAT	
21	36929000	36964000	36949320	36949327	+	59.2	TCACACAC	
21	36929000	36964000	36949760	36949767	-	55.5	ACACACCC	
21	36929000	36964000	36951248	36951255	+	61.7	TCACACTC	
21	36929000	36964000	36951646	36951653	+	100.0	TCACACCT	*
21	36929000	36964000	36952060	36952067	+	54.8	TCACAGCA	
21	36929000	36964000	36952725	36952732	-	77.2	ACACACCT	*
21	36929000	36964000	36952731	36952738	-	59.2	TCACACAC	*
21	36929000	36964000	36952736	36952743	+	57.3	TGACACCA	*
21	36929000	36964000	36952748	36952755	+	78.3	TCACACCC	*
21	36929000	36964000	36952762	36952769	+	60.5	ACACACTT	*
21	36929000	36964000	36952829	36952836	+	83.3	TCACACTT	*
21	36929000	36964000	36952921	36952928	-	52.9	TCACATAT	
21	36929000	36964000	36953072	36953079	-	77.2	ACACACCT	
21	36929000	36964000	36953184	36953191	-	56.4	AGACACCT	
21	36929000	36964000	36953906	36953913	+	77.2	ACACACCT	
21	36929000	36964000	36953949	36953956	-	58.1	ACACACAT	
21	36929000	36964000	36953951	36953958	-	59.2	TCACACAC	
21	36929000	36964000	36954424	36954431	+	51.3	TGACATCT	
21	36929000	36964000	36954474	36954481	+	55.9	TGACAGCT	
21	36929000	36964000	36954658	36954665	-	77.2	ACACACCT	
21	36929000	36964000	36956034	36956041	+	59.2	TCACACAC	
21	36929000	36964000	36956128	36956135	-	53.2	ACTCACCT	
21	36929000	36964000	36956161	36956168	+	60.5	ACACACTT	
21	36929000	36964000	36956187	36956194	+	56.4	AGACACCT	
21	36929000	36964000	36957174	36957181	+	52.9	TCACATAT	
21	36929000	36964000	36958185	36958192	-	83.3	TCACACTT	*
21	36929000	36964000	36958252	36958259	-	60.5	ACACACTT	*

21	36929000	36964000	36958278	36958285	-	57.3	TGACACCA	*
21	36929000	36964000	36958283	36958290	+	59.2	TCACACAC	*
21	36929000	36964000	36958289	36958296	+	77.2	ACACACCT	*
21	36929000	36964000	36960955	36960962	-	77.2	ACACACCT	
21	36929000	36964000	36961411	36961418	+	61.7	TCACACTC	
21	36929000	36964000	36961583	36961590	-	54.8	TCACAGCA	
21	36929000	36964000	36962019	36962026	-	80.9	TCACACAT	
21	36929000	36964000	36962880	36962887	-	60.5	ACACACTT	
21	36929000	36964000	36962890	36962897	-	58.1	ACACACAT	
21	36929000	36964000	36962959	36962966	+	52.6	TCTCAGCT	
21	36929000	36964000	36963846	36963853	+	61.7	TCACACTC	
21	36929000	36964000	36963954	36963961	-	61.7	TCACACTC	
25	11374000	11409000	11374093	11374100	-	59.0	TCACACAA	
25	11374000	11409000	11374140	11374147	+	62.5	TGACACTT	
25	11374000	11409000	11375064	11375071	-	59.3	TCTCACTT	
25	11374000	11409000	11375672	11375679	-	55.4	TCACATTT	
25	11374000	11409000	11375998	11376005	-	50.2	TCACATCA	
25	11374000	11409000	11378246	11378253	+	60.5	ACACACTT	
25	11374000	11409000	11378812	11378819	-	60.1	TGACACAT	
25	11374000	11409000	11379037	11379044	+	59.2	TCACACAC	
25	11374000	11409000	11379713	11379720	-	83.3	TCACACTT	
25	11374000	11409000	11379774	11379781	-	80.9	TCACACAT	
25	11374000	11409000	11380313	11380320	+	50.2	TCACATCA	
25	11374000	11409000	11380634	11380641	-	57.3	TGACACCA	
25	11374000	11409000	11380818	11380825	-	59.3	TCTCACTT	
25	11374000	11409000	11382630	11382637	-	55.4	TCACATTT	
25	11374000	11409000	11382846	11382853	-	72.0	TCACATCT	
25	11374000	11409000	11383368	11383375	-	100.0	TCACACCT	
25	11374000	11409000	11383457	11383464	+	50.2	TCACATCA	
25	11374000	11409000	11385436	11385443	-	83.3	TCACACTT	
25	11374000	11409000	11385805	11385812	-	59.0	TCACACAA	
25	11374000	11409000	11386512	11386519	-	60.5	ACACACTT	
25	11374000	11409000	11386528	11386535	-	62.5	TGACACTT	
25	11374000	11409000	11386649	11386656	+	60.0	TCACAGTT	
25	11374000	11409000	11386671	11386678	-	55.4	TCACATTT	
25	11374000	11409000	11386742	11386749	+	58.1	ACACACAT	
25	11374000	11409000	11387069	11387076	+	57.3	TGACACCA	*
25	11374000	11409000	11387985	11387992	-	79.2	TGACACCT	
25	11374000	11409000	11388062	11388069	+	52.9	TCACATAT	
25	11374000	11409000	11389022	11389029	-	58.1	ACACACAT	
25	11374000	11409000	11389642	11389649	+	79.2	TGACACCT	*
25	11374000	11409000	11389837	11389844	-	59.0	TCACACAA	*
25	11374000	11409000	11390563	11390570	+	60.1	TGACACAT	
25	11374000	11409000	11391722	11391729	-	55.0	TCACAGCC	

25	11374000	11409000	11391931	11391938	-	54.8	TCACAGCA	
25	11374000	11409000	11392669	11392676	+	54.1	TCTCACCA	
25	11374000	11409000	11392703	11392710	+	58.1	ACACACAT	
25	11374000	11409000	11392743	11392750	+	77.2	ACACACCT	
25	11374000	11409000	11393160	11393167	+	52.6	TCTCAGCT	*
25	11374000	11409000	11393507	11393514	-	100.0	TCACACCT	*
25	11374000	11409000	11393517	11393524	+	79.2	TGACACCT	*
25	11374000	11409000	11393635	11393642	-	80.9	TCACACAT	*
25	11374000	11409000	11394510	11394517	-	58.1	ACACACAT	
25	11374000	11409000	11395279	11395286	-	54.8	TCACAGCA	
25	11374000	11409000	11395641	11395648	+	54.8	TCACAGCA	
25	11374000	11409000	11395820	11395827	-	59.0	TCACACAA	
25	11374000	11409000	11396018	11396025	-	58.1	ACACACAT	
25	11374000	11409000	11396190	11396197	-	62.5	TGACACTT	
25	11374000	11409000	11396398	11396405	-	58.1	ACACACAT	*
25	11374000	11409000	11396538	11396545	-	55.3	ACACACCA	*
25	11374000	11409000	11396560	11396567	+	60.0	TCACAGTT	*
25	11374000	11409000	11396597	11396604	+	55.0	TCACAGCC	*
25	11374000	11409000	11396687	11396694	+	78.1	TCACACCA	*
25	11374000	11409000	11396742	11396749	+	59.0	TCACACAA	*
25	11374000	11409000	11396922	11396929	+	78.3	TCACACCC	
25	11374000	11409000	11397110	11397117	+	76.7	TCACAGCT	
25	11374000	11409000	11397612	11397619	-	61.5	TCACACTA	
25	11374000	11409000	11398176	11398183	+	60.5	ACACACTT	
25	11374000	11409000	11398539	11398546	-	58.1	ACACACAT	*
25	11374000	11409000	11398607	11398614	-	59.2	TCACACAC	*
25	11374000	11409000	11399755	11399762	-	54.3	TCTCACCC	
25	11374000	11409000	11400617	11400624	+	56.4	AGACACCT	*
25	11374000	11409000	11400705	11400712	+	54.3	TCTCACCC	*
25	11374000	11409000	11400798	11400805	+	55.0	TCACAGCC	*
25	11374000	11409000	11400979	11400986	-	61.7	TCACACTC	*
25	11374000	11409000	11401466	11401473	-	60.1	TGACACAT	
25	11374000	11409000	11401705	11401712	-	50.2	TCACATCA	
25	11374000	11409000	11401801	11401808	+	61.5	TCACACTA	
25	11374000	11409000	11402307	11402314	+	55.3	ACACACCA	
25	11374000	11409000	11402726	11402733	+	57.3	TGACACCA	
25	11374000	11409000	11402813	11402820	+	55.4	TCACATTT	
25	11374000	11409000	11403108	11403115	+	55.4	TCACATTT	
25	11374000	11409000	11403212	11403219	-	58.1	ACACACAT	
25	11374000	11409000	11403214	11403221	-	59.2	TCACACAC	
25	11374000	11409000	11404083	11404090	+	58.1	ACACACAT	
25	11374000	11409000	11404479	11404486	-	54.3	TCTCACCC	
25	11374000	11409000	11405325	11405332	+	55.5	ACACACCC	
25	11374000	11409000	11405362	11405369	+	61.5	TCACACTA	

25	11374000	11409000	11405827	11405834	-	100.0	TCACACCT	
25	11374000	11409000	11406440	11406447	-	55.4	TCACATTT	
25	11374000	11409000	11406938	11406945	-	57.3	TGACACCA	

Table S3. List of primers, antibodies and RNA probes

Morpholino sequences	
Ripply1	5'-CATCGTCACTGTGTTTTTCGTTTTG-3 (Kawamura et al., 2005)
Mesp-ba ATG	5'-TCGGTTCTTGCTTGAGGTTTGCATG-3' (Kawamura et al 2005)
Mesp-bb ATG	5'-CGTCCA TTCTGTGTGGTTGGAGA TT-3'
Mesp-ba splice	5'-TAACTTAACATACCTGGTACGGTGT-3'
Mesp-bb splice	5'-TTTAAAGCCTGTCTACACACCTGAT-3'
Standard control	5'-CCTCCTACCTCAGTTACAATTTATA-3'
p53 MO	5'-GCGCCATTGCTTTGCAAGAATTG-3' (Robu et al., 2007)

Primary antibodies	
Pax7, MF20, F59, cMyc	1:10, DSHB
Mef2	1:100, Santa Cruz
b-cat	1:1000, Sigma
Tbx6	1:250

Secondary antibodies	
Alexa-conjugated	1:800, Invitrogen

RNA probes	
meox	(Neyt et al., 2000)
mesp-ba	(Sawada et al., 2000)
mesp-bb	(Cutty et al., 2012)
myf5	(Coutelle et al., 2001)
myoD	(Weinberg et al., 1996)
pax3, pax7	(Seo et al., 1998)
ripply1, tbx6	(Kawahara et al., 2005)